Comparative morphometric study of obstetrical adaptations in primate skeleton including fetal stage

Mikaze KAWADA

2022

Contents

Abstract

Introduction

Acquisition of upright bipedalism shaped human pelvis in a unique way, which resulted in obstetrical difficulty. It is explained that humans are cornered into a dilemma: the obstetrical difficulty cannot be eased simply by expanding the pelvic dimensions since this "solution" could result in an increase of the energetic cost of bipedal locomotion. How then do humans resolve the problems of obstetrical difficulty? Besides a narrow birth canal of the mother, obstetrical difficulty is caused by the neonate that acquired a large head and wide shoulders. In this thesis, I address this question by conducting two studies that focus mainly on the head and shoulder morphologies and their development including the fetal stage, in light of obstetrical constraints:

1. *Covariation between the fetal skull and maternal pelvis*
   It has been proposed that the morphological covariation between the skull and pelvis (cephalopelvic covariation) alleviates the obstetrical difficulty in humans. However, the direct evidence of this proposition is lacking. I test this hypothesis using data of actual mother–fetus dyads at the perinatal phase of rhesus macaques as they exhibit a high cephalopelvic proportions comparable to humans.
2. *Shoulder development*
   Human skull has developmental features that are thought to evolve to ease obstetrical difficulties such as delayed fusion of the metopic suture. On the other hand, it remains unclear whether the development of human shoulders exhibit such adaptive developmental pattern. I address this question by comparing the shoulder growth patterns in human and nonhuman primate taxa that has different obstetrical difficulties.

Materials and Methods

Anesthetized or cadaveric subjects of humans, chimpanzees, and rhesus and Japanese macaques were scanned by medical computed tomography (CT) scanners, and three-dimensional surface data of skeleton were generated. Morphologies were then quantified by using landmark-based methods. The morphometric data of landmarks were then used to perform two-block partial least-squares (PLS) and visualization by means of thin-plate spline-based morphing (1st study), and to perform ontogenetic allometric analyses based on linear measurements of cranial dimensions, shoulder width, pelvic width, and lengths of the humerus and femur (2nd study).

Results and Discussion

Covariation between the fetal skull and maternal pelvis

This study provided the first direct evidence of morphological covariations between the fetal skull and maternal pelvis in primates. The covariation was observed mostly at the birth canal-related part of the maternal pelvis, and the morphologies of the birth canal and fetal skull covary in such a way that reduces the obstetrical difficulty. These results support the hypothesis that cephalopelvic covariation has evolved to alleviate the risk of obstructed labor.

Shoulder development

The ontogenetic data from the fetal to adult stages showed that clavicular growth was decelerated before birth but accelerated after birth in humans. Contrastingly, chimpanzees and Japanese macaques exhibited more uniform growth patterns of the clavicle. The pattern of prenatal deceleration and postnatal acceleration was found only in the clavicle of humans, but not in other skeletal parts of humans nor in other primates. These data indicate the development of the human shoulder is adaptive for obstetrical constraints.

These findings broaden our understanding of the evolution of childbirth in primates in two respects. First, evidence of cephalopelvic (and mother–fetus) covariation shows obstetrical adaptation is expressed not only in humans but also in other primates. Adaptative features to obstetrical constraint could have been acquired in various primate lineages independently or it could have appeared at the early catarrhine ancestor. In either case, it should be noted that humans are not special in terms of obstetrical adaptation. Second, inferred obstetrical adaptation in the shoulder development points that effects from obstetrical constraints are more pervasive on skeletal development in humans than previously thought.

Chapter 1
Introduction

Bipedality, big brain, wide shoulders, and childbirth

Humans (*Homo sapiens*) are distinguished from other extant mammals in various respects. In particular, the acquisition of bipedality with upright posture and encephalization are the hallmarks of human evolution. Combination of these two features resulted in the human-specific complication of childbirth. Childbirth links bipedality and encephalization via a fundamental locomotor and obstetrical skeletal part, the pelvis. Human pelvis is superoinferiorly short and antero-posteriorly deep (Fig. 1.1) due to adaptations to upright bipedality (Leutenegger, 1974; Lovejoy, 2005; Tague & Lovejoy, 1986), which resulted in small dimensions of the birth canal (Rosenberg & Trevathan, 1995; Schultz, 1949; Wittman & Wall, 2007). On the other hand, large brain at adult stage is associated with large brain at birth in humans [~400cc; (DeSilva, 2011; Foley et al., 1991)], which approximates the brain size in adult chimpanzees. Combination of cephalopelvic morphological changes caused a tight fit between maternal birth canal and fetal head (cephalopelvic disproportion).

Another major factor, other than the cephalopelvic disproportion, that complicates the human childbirth is the non-uniform shape of birth canal. The birth canal is medio-laterally wide at the inlet and midplane and is antero-posteriorly elongated at the outlet. Because the dimension of the neonatal head is largest along the antero-posterior direction, the human fetus rotates axially such that the largest diameter of the head matches the long diameter of birth canal at each plane (Rosenberg & Trevathan, 2002; Schultz, 1949; W. R. Trevathan, 1988, 2015; Wells et al., 2012). In addition to the axial rotation, human fetuses should flex and extend the neck to pass the birth canal that curves by ~90 degrees from caudal to abdominal directions (Fig. 1.1) (Abitbol, 1988; Bamberg et al., 2012; Myrfield et al., 1997; Rosenberg, 1992; W. R. Trevathan, 1988). In humans, the occipital part constitutes the largest portion of the neonatal skull. To fit the shape of skull to that of maternal birth canal, the human fetus should orient its occiput toward maternal pubis. The smallest dimension of neonatal head is the suboccipitobregmatic diameter. As a result of combination of the shapes of maternal birth canal and fetal skull, human neonates usually emerge from the birth canal with facing the dorsal direction of mothers and in occiput anterior position.

Another factor that caused human childbirth difficulty is the wide shoulder of humans. Although it draws less attention in evolutionary anthropological studies, shoulder dystocia, namely the arrest of the fetal shoulders in the birth canal, is not rare in humans (Ouzounian &

Gherman, 2005; Øverland et al., 2012). Shoulder dystocia can cause serious complications: On the neonatal side, it can lead asphyxia and/or brachial plexus injury that can lead to Erb's palsy (Gross et al., 1987; Sandmire & O'Halloin, 1988; Sjöberg et al., 1988); on the maternal side, it can lead to uterine rupture and/or excessive bleeding and, in the worst case, result in the death of neonates and/or mothers (Dajani & Magann, 2014; Gherman et al., 2006; W. R. Trevathan, 1988). Human fetuses need to rotate their shoulders to pass through the birth canal following the head (W. Trevathan & Rosenberg, 2000).

The tight fit between maternal birth canal and fetal head and shoulders results in obstetrical complications (Fig. 1.2). The duration for delivery is long in humans: in average, 12–18 hours in primiparas and 6–8 hours in multiparas (Artal-Mittelmark, 2021). Childbirth-related risk includes e.g., long-term damage of the pelvic organs on the maternal side (Royston et al., 1990) and oxygen deprivation, related brain damage, brachial plexus lesions, and infection on the fetal side (Dammann & Leviton, 2000; Hübler & Jorch, 2019). Mortality of mothers and/or neonates during or after delivery are considerably high in humans (WHO, 2014). As such, addressing obstetrical questions is of special relevance for understanding the human evolution.

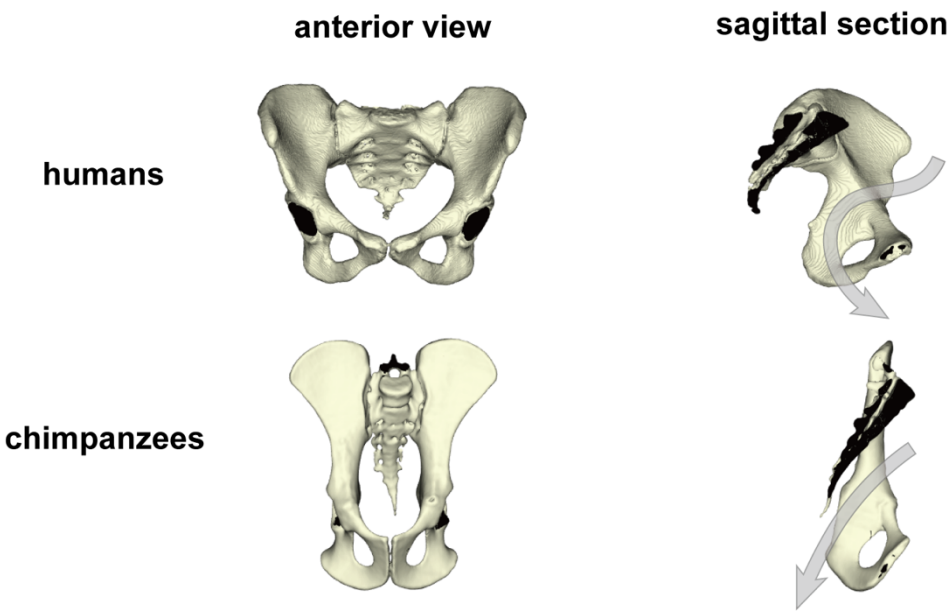

Fig. 1.1 Pelves of humans and chimpanzees. The pelvis of humans is overall rounded compared to that of chimpanzees. The gray arrows indicate the direction of the birth canal in humans and chimpanzees. Note the curved trajectory in humans.

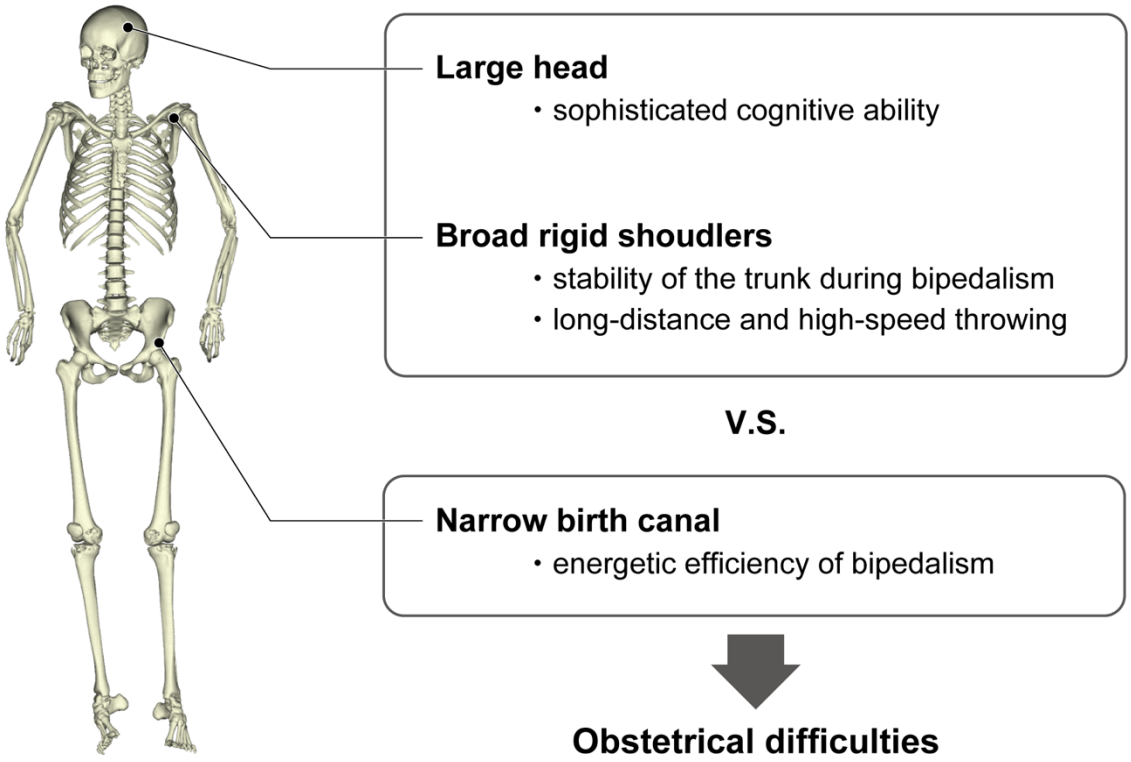

Fig. 1.2 Human skeleton and obstetrical difficulties. The large head and narrow birth canal are in evolutionary dilemma.

The obstetrical dilemma

Since Gregory (1928), it has been repeatedly asked why childbirth remains difficult for humans. Washburn (1960) proposed a hypothesis coined as "obstetrical dilemma" followed by numerous studies [e.g., Fischer and Mitteroecker (2015); Mitteroecker et al. (2016); Pavličev et al. (2020); Stansfield et al. (2021)]. A larger birth canal of mothers would reduce the obstetrical difficulties. According to the obstetrical dilemma hypothesis, this "solution" was not selected, since human pelvis is faced with a compromise between the delivery and bipedal locomotion (Rosenberg, 1992; Rosenberg & Trevathan, 2002; Ruff, 1995; Tague & Lovejoy, 1986; Wittman & Wall, 2007). Increasing the birth canal size, for example, the pelvic width and the distances between the sacroiliac and hip joints, would require greater muscular exertion to maintain the upright posture during bipedal locomotion and increase the energetic cost of locomotion (Rosenberg, 1992; Rosenberg & Trevathan, 1995; Ruff, 1995; Washburn, 1960; Wittman & Wall, 2007). How then about making the neonatal head smaller to ease obstetrical difficulties instead? There is a dilemma in this "solution", too. In humans, neonatal brain volumes and birth weight are strongly positively associated with infant survival rate (Alberman, 1991; Karn & Penrose, 1951; Zhang et al., 2008).

While the obstetrical dilemma hypothesis provides an excellent framework, this

hypothesis has been challenged on various grounds. First, an experimental study showed that locomotor cost is not increased in females compared to males even if females have a larger pelvis (relatively and absolutely) than males (Gruss et al., 2017; Rak, 1991; Wall-Scheffler & Myers, 2013, 2017; Warrener et al., 2015; Whitcome et al., 2017). Second, the hypothesis has been challenged from a perspective that pregnancy is energetically demanding for mothers. According to the hypothesis of "energetics of gestation and growth", size of the neonatal head and associated pelvic dimensions are restricted by metabolically constrained gestation length rather than by the locomotor economy (Dunsworth et al., 2012).

Childbirth in non-human primates

It is often mentioned that the human childbirth is "unique." Do we actually know that human childbirth is truly unique? To answer this question, data from other primates are essential. Actualistic data of childbirth in non-human primates are still scarce though its importance is acknowledged (Rosenberg, 1992; Rosenberg & Trevathan, 1995). The relationship between the sizes of maternal birth canal and neonatal head are known. As a result of allometric scaling, the smaller the mothers are, the larger the neonates are relative to their mothers (DeSilva, 2011; DeSilva & Lesnik, 2008; Schultz, 1949). Thus, large-bodied non-human primates (e.g., orangutans, chimpanzees, and gorillas) and small- to middle-bodied primates (e.g., marmosets, squirrel monkeys, macaques, and gibbons) have low and high cephalopelvic proportions, respectively, of which the cephalopelvic proportion is comparable to humans in the latter (Fig. 1.3) (DeSilva, 2011; DeSilva & Lesnik, 2008; Schultz, 1949).

The birth mechanism differs between humans and non-human primates. In all primates, the birth canal is composed of three planes, the inlet, midplane, and outlet. In non-human primates, the sagittal diameter of the birth canal is largest in all planes. The neonatal cranium has the largest dimension sagittally. It had been assumed that in non-human primates fetuses pass through the straight birth canal without some rotations. However, Stoller (1996) showed that fetal rotation is required in squirrel monkeys (*Saimiri sciureus*) and baboons (*Papio anubis*). Stoller observed deliveries in seven squirrel monkeys and four baboons using X-ray radiographies and found that fetuses extended their necks to exit with their face first (mentum anterior) showing different patterns of fetal rotation from humans.

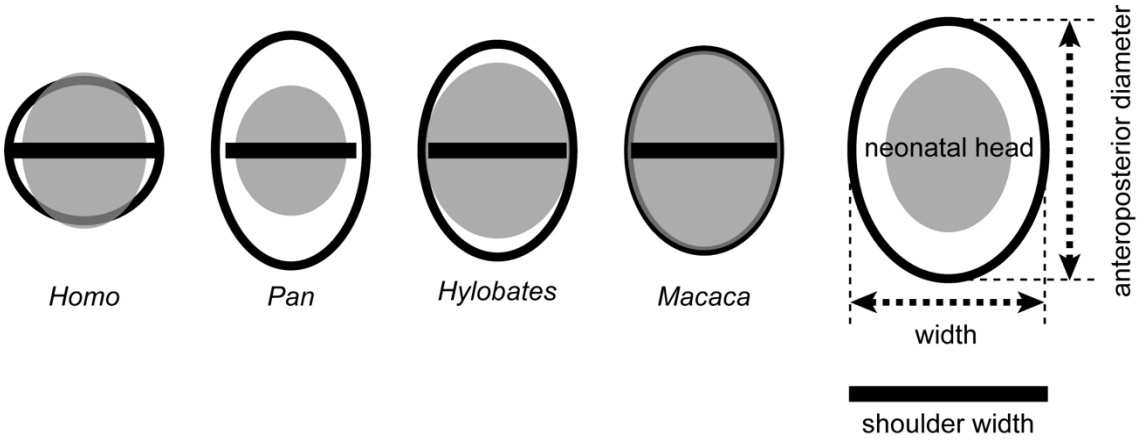

Fig. 1.3 Proportions between the dimensions of maternal pelvic inlet and neonatal skull and shoulders. Note the high cephalopelvic proportion in *Macaca* that is comparable to humans. In chimpanzees, the neonates are comparatively small relative to the maternal birth canal. [drawing based on Schultz (1949)].

The unresolved issues

Recently, Fischer and Mitteroecker (2015) put forth the hypothesis that morphological covariation between the fetal skull and maternal pelvis (cephalopelvic covariation) alleviates the risk of obstructed labor in humans, adding another line of argument on the obstetrical dilemma hypothesis in humans. However, their hypothesis is yet to be tested by critical data to substantiate their theory, that is actual mother–fetus dyad skeletal dimensions. In addition, shoulders, which is another factor of obstetrical difficulties in humans, are largely "forgotten." Current knowledge is limited to interspecific comparison of the proportion between female pelvic dimension and neonatal shoulder width (Schultz, 1949). In this thesis, I address the following questions:

1. *Does the morphological covariation between the fetal skull and maternal pelvis alleviate obstetrical difficulty?*

   Fischer and Mitteroecker (2015) used the within-individual covariation between the pelvic shape and head size in female to infer the fetopelvic relationships. I investigate data of the actual mother–fetus dyads during the perinatal period of rhesus macaques, a species which has high cephalopelvic proportion comparable to humans.

2. *Is human shoulder development adapted to obstetrical constraints?*

   It is well known that the human skull has various developmental features that are thought to be adapted to obstetrical constraints such as the relatively small head of neonates compared with adults and the delayed fusion of the metopic suture. On the other hand, it remains

unexplored whether the shoulder exhibits similar adaptive features. I address this question by comparing the developmental patterns from fetal to adult stage in humans, chimpanzees, and Japanese macaques, which have different obstetrical conditions.

References

Abitbol, M. M. (1988). Evolution of the ischial spine and of the pelvic floor in the hominoidea. *American Journal of Physical Anthropology, 75*(1), 53-67. doi:10.1002/ajpa.1330750107

Alberman, E. (1991). Are our babies becoming bigger? *Journal of the Royal Society of Medicine, 84*(5), 257-260.

Artal-Mittelmark, R. (2021). Stages of development of the fetus-women's health issues. In: Merck Manuals Consumer Version. Retrieved from https://www.merckmanuals.com/home/women-s-health-issues/normal-pregnancy/stages-of-development-of-the-fetus#v809193.

Bamberg, C., Rademacher, G., Güttler, F., Teichgräber, U., Cremer, M., Bührer, C., Spies, C., Hinkson, L., Henrich, W., Kalache, K. D., & Dudenhausen, J. W. (2012). Human birth observed in real-time open magnetic resonance imaging. *American Journal of Obstetrics and Gynecology, 206*(6), 505.e501-505.e506. doi:https://doi.org/10.1016/j.ajog.2012.01.011

Dajani, N. K., & Magann, E. F. (2014). Complications of shoulder dystocia. *Seminars in Perinatology, 38*(4), 201-204. doi:https://doi.org/10.1053/j.semperi.2014.04.005

Dammann, O., & Leviton, A. (2000). Role of the fetus in perinatal infection and neonatal brain damage. *Current Opinion in Pediatrics, 12*(2), 99-104.

DeSilva, J. M. (2011). A shift toward birthing relatively large infants early in human evolution. *Proceedings of the National Academy of Sciences, 108*(3), 1022-1027. doi:10.1073/pnas.1003865108

DeSilva, J. M., & Lesnik, J. J. (2008). Brain size at birth throughout human evolution: A new method for estimating neonatal brain size in hominins. *Journal of Human Evolution, 55*(6), 1064-1074. doi:https://doi.org/10.1016/j.jhevol.2008.07.008

Dunsworth, H. M., Warrener, A. G., Deacon, T., Ellison, P. T., & Pontzer, H. (2012). Metabolic hypothesis for human altriciality. *Proceedings of the National Academy of Sciences,*

109(38), 15212-15216. doi:10.1073/pnas.1205282109

Fischer, B., & Mitteroecker, P. (2015). Covariation between human pelvis shape, stature, and head size alleviates the obstetric dilemma. *Proceedings of the National Academy of Sciences, 112*(18), 5655-5660. doi:10.1073/pnas.1420325112

Foley, R. A., Lee, P. C., Widdowson, E. M., Knight, C. D., Jonxis, J. H. P., Widdowson, E. M., Whiten, A., & Bone, Q. (1991). Ecology and energetics of encephalization in hominid evolution. *Philosophical Transactions of the Royal Society of London. Series B: Biological Sciences, 334*(1270), 223-232. doi:doi:10.1098/rstb.1991.0111

Gherman, R. B., Chauhan, S., Ouzounian, J. G., Lerner, H., Gonik, B., & Goodwin, T. M. (2006). Shoulder dystocia: The unpreventable obstetric emergency with empiric management guidelines. *American Journal of Obstetrics and Gynecology, 195*(3), 657-672. doi:https://doi.org/10.1016/j.ajog.2005.09.007

Gregory, W. K. (1928). The upright posture of man: A review of its origin and evolution. *Proceedings of the American Philosophical Society, 67*(4), 339-377.

Gross, T. L., Sokol, R. J., Williams, T., & Thompson, K. (1987). Shoulder dystocia: A fetal-physician risk. *American Journal of Obstetrics and Gynecology, 156*(6), 1408-1418. doi:https://doi.org/10.1016/0002-9378(87)90008-1

Gruss, L. T., Gruss, R., & Schmitt, D. (2017). Pelvic breadth and locomotor kinematics in human evolution. *The Anatomical Record, 300*(4), 739-751. doi:https://doi.org/10.1002/ar.23550

Hübler, A., & Jorch, G. (2019). *Neonatologie: Die medizin des früh-und reifgeborenen*: Georg Thieme Verlag.

Karn, M. N., & Penrose, L. S. (1951). Birth weight and gestation time in relation to maternal age, parity and infant survival. *Annals of Eugenics, 16*(1), 147-164. doi:https://doi.org/10.1111/j.1469-1809.1951.tb02469.x

Leutenegger, W. (1974). Functional aspects of pelvic morphology in simian primates. *Journal of Human Evolution, 3*(3), 207-222. doi:https://doi.org/10.1016/0047-2484(74)90179-1

Lovejoy, C. O. (2005). The natural history of human gait and posture: Part 1. Spine and pelvis. *Gait & Posture, 21*(1), 95-112. doi:https://doi.org/10.1016/j.gaitpost.2004.01.001

Mitteroecker, P., Huttegger, S. M., Fischer, B., & Pavlicev, M. (2016). Cliff-edge model of

obstetric selection in humans. *Proceedings of the National Academy of Sciences, 113*(51), 14680-14685. doi:doi:10.1073/pnas.1612410113

Myrfield, K., Brook, C., & Creedy, D. (1997). Reducing perineal trauma: implications of flexion and extension of the fetal head during birth. *Midwifery, 13*(4), 197-201. doi:https://doi.org/10.1016/S0266-6138(97)80006-X

Ouzounian, J. G., & Gherman, R. B. (2005). Shoulder dystocia: Are historic risk factors reliable predictors? *American Journal of Obstetrics and Gynecology, 192*(6), 1933-1935. doi:https://doi.org/10.1016/j.ajog.2005.02.054

Øverland, E. A., Vatten, L. J., & Eskild, A. (2012). Risk of shoulder dystocia: associations with parity and offspring birthweight. A population study of 1 914 544 deliveries. *Acta Obstetricia et Gynecologica Scandinavica, 91*(4), 483-488. doi:https://doi.org/10.1111/j.1600-0412.2011.01354.x

Pavličev, M., Romero, R., & Mitteroecker, P. (2020). Evolution of the human pelvis and obstructed labor: new explanations of an old obstetrical dilemma. *American Journal of Obstetrics & Gynecology, 222*(1), 3-16. doi:10.1016/j.ajog.2019.06.043

Rak, Y. (1991). Lucy's pelvic anatomy: its role in bipedal gait. *Journal of Human Evolution, 20*(4), 283-290. doi:https://doi.org/10.1016/0047-2484(91)90011-J

Rosenberg, K. (1992). The evolution of modern human childbirth. *American Journal of Physical Anthropology, 35*(S15), 89-124. doi:10.1002/ajpa.1330350605

Rosenberg, K., & Trevathan, W. (1995). Bipedalism and human birth: The obstetrical dilemma revisited. *Evolutionary Anthropology: Issues, News, and Reviews, 4*(5), 161-168. doi:10.1002/evan.1360040506

Rosenberg, K., & Trevathan, W. (2002). Birth, obstetrics and human evolution. *BJOG: An International Journal of Obstetrics & Gynaecology, 109*(11), 1199-1206. doi:10.1046/j.1471-0528.2002.00010.x

Royston, E., Armstrong, S., & Organization, W. H. (1990). *La prévention des décès maternels*: Organisation mondiale de la Santé.

Ruff, C. B. (1995). Biomechanics of the hip and birth in early *Homo*. *American Journal of Physical Anthropology, 98*(4), 527-574. doi:10.1002/ajpa.1330980412

Sandmire, H. F., & O'Halloin, T. J. (1988). Shoulder dystocia: its incidence and associated risk factors. *International Journal of Gynecology & Obstetrics, 26*(1), 65-73. doi:https://doi.org/10.1016/0020-7292(88)90198-1

Schultz, A. H. (1949). Sex differences in the pelves of primates. *American Journal of Physical Anthropology, 7*(3), 401-424. doi:10.1002/ajpa.1330070307

Sjöberg, I., Erichs, K., & BJerre, I. (1988). Cause and effect of obstetric (neonatal) brachial plexus palsy. *Acta Paediatrica, 77*(3), 357-364. doi:https://doi.org/10.1111/j.1651-2227.1988.tb10660.x

Stansfield, E., Kumar, K., Mitteroecker, P., & Grunstra, N. D. S. (2021). Biomechanical trade-offs in the pelvic floor constrain the evolution of the human birth canal. *Proceedings of the National Academy of Sciences, 118*(16), e2022159118. doi:doi:10.1073/pnas.2022159118

Stoller, M. K. (1996). The obstetric pelvis and mechanism of labor in nonhuman primates.

Tague, R. G., & Lovejoy, C. O. (1986). The obstetric pelvis of A.L. 288-1 (Lucy). *Journal of Human Evolution, 15*(4), 237-255. doi:https://doi.org/10.1016/S0047-2484(86)80052-5

Trevathan, W., & Rosenberg, K. (2000). The shoulders follow the head: postcranial constraints on human childbirth. *Journal of Human Evolution, 39*(6), 583-586. doi:https://doi.org/10.1006/jhev.2000.0434

Trevathan, W. R. (1988). Fetal emergence patterns in evolutionary perspective. *American Anthropologist, 90*(3), 674-681. doi:10.1525/aa.1988.90.3.02a00100

Trevathan, W. R. (2015). Primate pelvic anatomy and implications for birth. *Philosophical Transactions of the Royal Society B: Biological Sciences, 370*(1663), 20140065. doi:10.1098/rstb.2014.0065

Wall-Scheffler, C. M., & Myers, M. J. (2013). Reproductive costs for everyone: How female loads impact human mobility strategies. *Journal of Human Evolution, 64*(5), 448-456. doi:https://doi.org/10.1016/j.jhevol.2013.01.014

Wall-Scheffler, C. M., & Myers, M. J. (2017). The biomechanical and energetic advantages of a mediolaterally wide pelvis in women. *The Anatomical Record, 300*(4), 764-775. doi:10.1002/ar.23553

Warrener, A. G., Lewton, K. L., Pontzer, H., & Lieberman, D. E. (2015). A wider pelvis does not increase locomotor cost in humans, with implications for the evolution of childbirth. *PLOS ONE, 10*(3), e0118903. doi:10.1371/journal.pone.0118903

Washburn, S. L. (1960). Tools and human evolution. *Scientific American, 203*(3), 62-75.

Wells, J. C. K., DeSilva, J. M., & Stock, J. T. (2012). The obstetric dilemma: An ancient game of Russian roulette, or a variable dilemma sensitive to ecology? *American Journal of Physical Anthropology, 149*(S55), 40-71. doi:10.1002/ajpa.22160

Whitcome, K. K., Miller, E. E., & Burns, J. L. (2017). Pelvic rotation effect on human stride length: releasing the constraint of obstetric selection. *The Anatomical Record, 300*(4), 752-763. doi:https://doi.org/10.1002/ar.23551

WHO. (2014). *Trends in maternal mortality: 1990 to 2013: estimates by WHO, UNICEF, UNFPA, The World Bank and the United Nations Population Division: executive summary*. Retrieved from

Wittman, A. B., & Wall, L. L. (2007). The evolutionary origins of obstructed labor: Bipedalism, encephalization, and the human obstetric dilemma. *Obstetrical & Gynecological Survey, 62*(11), 739-748. doi:10.1097/01.ogx.0000286584.04310.5c

Zhang, X., Decker, A., Platt, R. W., & Kramer, M. S. (2008). How big is too big? The perinatal consequences of fetal macrosomia. *American Journal of Obstetrics and Gynecology, 198*(5), 517.e511-517.e516. doi:https://doi.org/10.1016/j.ajog.2007.12.005

Chapter 2

Covariation of fetal skull and maternal pelvis during the perinatal period in rhesus macaques and evolution of childbirth in primates

Published in: *Proceedings of the National Academy of Sciences* 117 (35): 21251-21257

Introduction

Encephalization and acquisition of bipedal locomotion are hallmarks of human evolution. In modern humans, adult and neonatal brain volumes reach 1,400 cc and 400 cc on average, respectively (DeSilva, 2011; Foley et al., 1991; Gibson, 2002). Bipedality with upright posture shaped the human pelvis in a specific way compared to other primates. The human pelvis is short and deep along the cephalocaudal and dorsoventral directions, respectively, which is thought to be associated with the stability and efficiency of bipedal locomotion (W. Leutenegger, 1974; Lovejoy, 2005; Tague & Lovejoy, 1986). The human pelvic morphology results in a narrow birth canal especially along the anteroposterior direction at the pelvic inlet (Rosenberg & Trevathan, 1995; Adolph H. Schultz, 1949; Wittman & Wall, 2007). As a result of encephalization and adaptations for bipedalism, neonatal head and maternal pelvic dimensions typically exhibit a tight fit in humans. The large human neonatal head relative to maternal pelvic sizes (a high cephalopelvic proportion) frequently leads to difficulties in childbirth, and has prompted a unique delivery process coupled with fetal rotation (Rosenberg & Trevathan, 2002; Adolph H. Schultz, 1949; Wenda R. Trevathan, 1988, 2015; Wells et al., 2012) [but see Hirata et al. (2011); Stoller (1996)].

In principle, the risks of obstructed labor should be reduced by expanding true pelvic dimensions (Correia et al., 2005; W. Leutenegger, 1974; Rosenberg, 1992; Rosenberg & Trevathan, 1995; Wittman & Wall, 2007). There is a limitation in the capacity of pelvic expansion, however, since increased pelvic width hampers energetic efficiency of bipedal locomotion (Rosenberg, 1992; Rosenberg & Trevathan, 1995; Ruff, 1995; Wittman & Wall, 2007) [but see (Dunsworth et al., 2012; Warrener et al., 2015)]. Such a trade-off that was hypothesized for the human pelvis is known as the “obstetric dilemma” (Dunsworth et al., 2012; Huseynov et al., 2016; Krogman, 1951; Walter Leutenegger, 1982; Roberts & Thorpe, 2014; Rosenberg & Trevathan, 1995; Ruff, 1995; Adolph H. Schultz, 1949; Washburn, 1960). This long-standing hypothesis was recently challenged by Warrener et al. (2015) who showed that the broader pelves of females compared to males do not result in energetic inefficiency. In either case, the expansion of pelvic dimensions is limited, since a pelvic floor that is too large could increase risk of visceral prolapse (Sze et al., 1999).

Given the relatively large head of the human neonate and the constrained pelvic width for efficient bipedalism, what could then reduce the risk of obstructed labor? Do the morphologies of the skull and pelvis covary and co-evolve to reduce difficulty of childbirth? As the delivery process itself is primarily determined by the interaction between the fetal head and maternal pelvis, the morphological covariation between the head and pelvis [cephalopelvic covariation (CPC)] has

drawn considerable attention. It has been reported that the sizes of the neonatal and maternal heads show a positive correlation in humans (Gilmore et al., 2010; Smit et al., 2010). Fischer and Mitteroecker (2015) showed that humans with larger heads tend to exhibit a rounder shape of the pelvic inlet with greater projection of the shorter sacrum to the dorsal direction and the larger anteroposterior diameter in the pelvic outlet. They also showed that such covariation between the head size and pelvic shape is stronger in females than in males. Based on these data, they proposed that the morphologies of the skull and pelvis covary to ease childbirth.

Small-to-middle-sized primates (e.g., marmosets, squirrel monkeys, macaques, and gibbons) also tend to exhibit high cephalopelvic proportions (Adolph H. Schultz, 1949) since maternal body mass and neonatal body and brain masses follow negative allometry (DeSilva, 2011; DeSilva & Lesnik, 2008). In these taxa, the frequency of neonatal death during the childbirth is relatively high (W. Leutenegger, 1974; Walter Leutenegger, 1982; Wenda R. Trevathan, 1988). It is currently unknown whether the CPC evolved only in humans, in parallel in other primate taxa, or is a shared anthropoid synapomorphy. Addressing this question is of special relevance to infer the evolutionary history of the CPC in primates. Here, we assess the CPC in *Macaca*, a genus that exhibits a high cephalopelvic proportion. The macaques exhibit a high cephalopelvic proportion comparable to humans (Adolph H. Schultz, 1949; Adolph Hans Schultz, 1969; Wenda R Trevathan, 2017), but do not exhibit obligate bipedalism. Investigating the CPC in macaques could thus provide new insights into the CPC hypothesis proposed by Fischer and Mitteroecker (2015).

While the CPC is the key for understanding the evolution of the delivery processes in ptimates, our current knowledge is limited in two aspects: First, direct data on the CPC are still scarce [but see Hirata et al. (2011)]. Fischer and Mitteroecker (2015) proposed the hypothesis based on the within-individual covariation of the skull and pelvis in adults. However, the morphology of the neonatal head is determined not only by the maternal but also by the paternal genetic factors. Thus, direct phenotypic data of the mother and its fetus are essential. Second, data on the covariation of the three-dimensional neonatal skull and maternal pelvic morphology remain unexplored. In this study, we investigate the CPC using direct data obtained from mother−fetus dyads of rhesus macaques (*Macaca mulatta*) (Fig. 2.1, SI, Figs S2.1, S2.2, S2.3, Table S2.1). We obtained detailed skeletal morphological data derived from computed tomography (CT) scans of perinatal rhesus macaques, such that the fetal skull remains physically intact.

We analyze the CPC using the following framework: First, we identify how the fetal head passes through the birth canal using the in-silico simulation. Specifically, we evaluate whether any head rotation is required for the fetuses to pass through the birth canals. In macaques,

the diameter of the birth canal is larger dorsoventrally than mediolaterally throughout the birth canal (Adolph H. Schultz, 1949; Adolph Hans Schultz, 1969; Tague, 1991; Washburn, 1942), while directions of long axes of birth canal diameters differ at the pelvic inlet and outlet in humans (Lovejoy, 2005; Rosenberg, 1992; Rosenberg & Trevathan, 1995, 2002). The pattern of fetal rotation in macaques could thus differ from that in humans. We virtually moved the three-dimensional surface model of the fetal head relative to that of the maternal pelvis in each of the actual mother−fetus dyads, minimizing contact between the fetal head and maternal pelvis (see also Materials and Methods). Second, we ask whether the fetal skull and maternal pelvis show the covariation of three-dimensional morphologies (H0). If H0 is supported, we then ask whether the CPC corresponds to childbirth rather than to other functions, such as locomotion (H1), and whether the CPC reduces the obstruction of childbirth in rhesus macaques (H2). To answer these questions, we assess the three-dimensional morphologies of the fetal skull and maternal pelvis using geometric morphometrics.

Materials and Methods

CT scanning

Using a medical CT scanner (Asteion, Cannon Medical Systems, Otawara, Japan), we scanned twelve rhesus macaque mother−fetus dyads, of which two mothers were scanned twice with different fetuses in different years (SI, Table S2.1). Due to the difficulty in obtaining data of mother−fetus dyads, we counted the data from these two mothers as independent datasets. The rhesus macaques used in this study were all raised at the Primate Research Institute of Kyoto University (KUPRI). All CT scans were performed at KUPRI. The CT scans used here were registered and are available via the website of the Digital Morphology Museum of KUPRI (http://dmm.pri.kyoto-u.ac.jp/dmm/WebGallery/index.html).

Mothers were anesthetized by A.K. before CT scans using one of the following protocols: intramuscularly with 10 mg ketamine hydrochloride (Ketalar ®; Daiichi Sankyo Propharma, Tokyo, Japan), 0.01 mg atropine sulfate hydrate (Atropine Injection 0.05%,® Terumo, Tokyo, Japan) per kilogram of body weight; or intramuscularly with 8 mg ketamine hydrochloride, or 0.0125 mg medetomidine hydrochloride (Domitor®; Nippon Zenyaku Kogyo, Fukushima, Japan). Note that method of anesthetization does not affect quality of resulting images of CT scans. While the subjects were under anesthesia, the pulse rate and SpO2 (an estimate of arterial oxygen saturation) were monitored using a medical monitor (BP-608EV, Fukuda Colin Co. Ltd, Tokyo, Japan). Respiration was checked visually. After all the scanning procedures were completed, subjects that were anesthetized with medetomidine hydrochloride were awakened by an

intramuscular injection of 0.03125 mg atipamezole (Mepatia; Meiji, Tokyo, Japan) per kilogram of body weight.

The CT scanning and image reconstruction parameters are as follows: beam collimation 1.0 mm, pitch: 0.75, reconstruction interval: 0.3−0.5 mm, reconstruction kernel: FC30 or FC31. We controlled the timing of the scan during pregnancy as much as possible, but each dataset has different lengths of time lags between the dates of CT scan and birth which varied from 8 to 37 days (SI, Table S2.1). In ten out of twelve cases, the fetal head was oriented toward the caudal direction of the mother (SI, Fig. S2.1). The CT volumetric data were then converted into surface models using Amira (Thermo Fisher Scientific, ver. 5.50). All experiments were performed in strict accordance with the Guidelines for the Care and Use of Laboratory Primates at KUPRI (third edition) (Primate Research Institute, 2010). The protocol was approved by the Animal Welfare and Animal Care Committee at KUPRI (permit numbers: 2013-004, 2015-004, 2018-018, 2020-156)

Morphometric data acquisition and analysis

The three-dimensional surface models of mother−fetus dyads derived from CT data were imported to an in-house program, ForMATit, developed by N.M. [MATLAB-based (Mathworks, ver. R2019b)]. The surface models were separated into mothers and fetuses to perform the in-silico simulation of childbirth. Various positions and orientations of the fetal head relative to the maternal pelvis were simulated for all the dyads (Fig. 2.1, SI, Figs. S2.4, S2.5).

The three-dimensional morphology was quantified using landmarks (SI, Fig. S2.6; a total of 74 and 59 landmarks for the skull and pelvis, respectively) using ForMATit. The landmark locations were determined following Morimoto et al. (2008) for the fetal skull, and Moffett (2017) and Christoph P.E. Zollikofer et al. (2017) for the maternal pelvis. See SI, Tables S2.2 and S2.3 for landmark definitions. The overall sizes of the fetal skull and maternal pelvis were evaluated by the centroid size calculated from landmark coordinate data (Bookstein, 1991). In this study, we focus on the form (size and shape) of the fetal skull and maternal pelvis. Thus, the following analyses of the morphological covariation were performed without size standardization.

The morphological covariation was evaluated by two-block PLS (partial least-squares) (Rohlf & Corti, 2000) following the protocols in Klingenberg (2009) and Zelditch et al. (2012). The differences in position and orientation of landmark configuration were corrected using Generalized Procrustes fitting for each skull and pelvis. The level of covariation between two sets (blocks) of data (here, landmark configurations of the skull and pelvis) was evaluated by RV coefficient (Escoufier, 1973) calculated using the variance−covariance matrix within each block

and covariance matrix between the two blocks. Note that RV is an extension of the expression for the squared correlation coefficient (Klingenberg, 2009). The level of significance of RV was evaluated using the permutation test (10,000 permutations); that is, a comparison of the RV coefficient for actual mother−fetus dyads and that of randomly generated dyads, testing whether the observed covariation is obtained by chance. The p-value was calculated as the number of RV_{random} that is larger than RV_{real}, divided by the total number of permutations (Klingenberg, 2009).

The contribution ratio of PLS1-related variation to the total variation, which we call PLSC (PLS-contribution) score, was calculated for each landmark as

$$PLSC_i = \frac{\sum_{x,y,z} var(coord_{i,PLS1})}{\sum_{x,y,z} var(coord_{i,Proc})}$$

where i denotes the landmark number on the maternal pelvis (i = 1, 2, …, 59), var denotes the function to calculate the variance, and $coord_{Proc}$ and $coord_{PLS1}$ denote Cartesian coordinates that were processed by Generalized Procrustes fitting and were reconstructed from the PLS1 score for each individual, respectively [thus the PLSC score at each landmark was calculated from twelve (i.e., sample size of mothers) data points]. We then tested whether the PLSC score differs between the birth canal and other locations using the Wilcoxon rank sum test (see SI, Fig. S2.6 for definition of birth canal-related landmarks). The PLSC score and variation of landmark coordinates were also visualized as spheres of different sizes plotted on the surface model (Fig. 2.3).

The morphological variation along the PLS1 axis was visualized for the fetal skull and maternal pelvis as deformations of the surface models at maximum and minimum values of the PLS1 score. The surface models of the skull and pelvis were used as templates for deformation, according to the different landmark configurations using thin-plate spline function (Christoph P. E. Zollikofer & León, 2002). A dyad, which was close to the average of all individuals, was selected as the template for deformation [IDs: PRI-Mm-1565 (mother) and PRI-Mm-2034 (fetus)]. All the calculations were performed using MATLAB.

Results

In all the mother−fetus dyads examined in this study, the anteroposterior diameter (see SI, Fig. S2.7 for definition) of the fetal skull was considerably larger than the dorsoventral diameter of the pelvic outlet, and the fetal skull width was considerably larger than the mediolateral diameter of the pelvic outlet (SI, Table S2.4, Figs. 1, S2.4, S2.5). Specifically, the mediolateral diameter of the birth canal is smallest at the ischial spines (Fig. 2.1, SI, Figs. S2.7, S2.4, S2.5). Thus, the major

constraint of childbirth in rhesus macauqes is the disproportion of the mediolateral diameters of both the fetal cranium and the pelvic outlet. The in-silico simulation shows that the space between the head and birth canal is larger when the fetal face is oriented toward the caudal direction than when it is oriented toward the pubic direction of the mother in all the dyads (Fig. 2.1BC, SI, Figs. S2.4, S2.5). When the fetal face is oriented toward the pubic direction of the mother, there are more "crash points" between the fetal skull and maternal pelvis (Fig. 2.1B, SI, Fig. S2.5). While there are extra spaces ventral and dorsal to the fetal head when the fetal face is oriented toward the caudal direction of the mother (Fig. 2.1C, SI, Fig. S2.4), further movement and/or rotation of the fetal head is considerably limited (SI, Fig. S2.4). To minimize the contact of the fetal head and maternal pelvis, the midsagittal planes of the maternal pelvis and fetal skull should, in principle, overlap and the fetal head should pass though the center of the birth canal (Fig. 2.1C). Thus, it appears that a rotation during childbirth, with which the fetal head is in oblique or transverse positions relative to the maternal pelvis, is not likely in most of the dyads (eleven out of twelve; see SI, Fig. S2.4).

To test these hypotheses, we quantified the three-dimensional morphologies of the fetal skull and maternal pelvis by anatomical points of reference (so-called landmarks) (SI, Fig. S2.6). According to H0, actual mother−fetus dyads should show a higher level of morphological covariation than random combinations of mothers and fetuses. This can be tested using two-block PLS (partial least-squares) (Rohlf & Corti, 2000). According to H1, the magnitude of the covariation should be greater at locations within the birth canal than other locations of the pelvis. The birth canal of rhesus macaques consists of the linea terminalis (the ilium, upper part of the sacrum, and upper part of the pubis; inlet), ischium, sacrum, and pubis (midplane), and the lower part of the ischium and the lower part of the sacrum (outlet). In contrast to humans, the pelvic outlet in non-human primates is located dorsal to the ischial tuberosities (Berge et al., 1984; Wenda R. Trevathan, 1988). Thus, the location of the ischial tuberosities, as well as the ischial spines, should be closely associated with difficulty of childbirth in rhesus macaques. Finally, if the CPC reduces the obstruction during childbirth (H2), then locations of the fetal skull and maternal pelvis, especially the birth canal, that contribute to CPC should correspond to each other. For example, it is expected that the covariation will be observed between the overall morphologies of the fetal skull and maternal pelvis; i.e., mothers with birth canals of circular vs. elliptic cross-sectional shape should have fetuses with globular vs. ellipsoidal skulls, respectively.

Test of H0: In this study, we focus on the variation in form (size and shape) (Bookstein, 1991). The results of two-block PLS show that the fetal skull and maternal pelvis exhibit a relatively high level of covariation [RV = 0.60; p = 0.02, level of significance was tested by 10,000

permutations; see Fig. 2.2 for PLS1 scores] (see Materials and Methods).

Test of H1: We then evaluated the contribution ratio of each landmark coordinate to PLS1 in the maternal pelvis, which was calculated as the proportion of PLS1-related variance to the entire variance of the coordinate for each landmark [henceforth PLSC (PLS-contribution) score]. The PLSC score is statistically higher at birth canal-related landmarks than at other landmarks ($p = 0.01$, Wilcoxon rank sum test). The visualization of the landmark-specific PLSC score (Fig. 2.3) shows that the contribution ratio is relatively high, especially at the pelvic inlet (e.g. on the pelvic brim, pubic region, and sacral promontory) and at outlet (e.g. on the medial parts of the pelvic tuberosities and ischial spines). In contrast, the PLSC is relatively low on the lateral parts of the ilium and ischium, which are not directly related to the morphology of the birth canal.

Test of H2: The morphologies corresponding to highest and lowest PLS1 scores (PLSmax and PLSmin, respectively) were visualized using thin-plate spline-based morphing of the three-dimensional surface models for the fetal skull and maternal pelvis (Fig. 2.4). PLSmax and PLSmin correspond to the small and large sizes of the fetal skull and maternal pelvis, respectively. The visualization of PLS1-related morphological variations is summarized as follows.

Skull: The width of the fetal skull is fairly constant for the PLSmax and PLSmin fetal skulls despite the difference in their overall sizes (Fig. 2.4A). Thus, the overall shape of the PLSmax (small) skull is rounded due to relatively large mediolateral diameter, while that of the PLSmin (large) is anteroposteriorly and superoinferiorly elongated (Fig. 2.4A; see SI, Fig. S2.8 for measurements of the skull width relative to the overall skull size). Thus, the size variation of the fetal skull is largely due to variation of the length and height, while the skull width remains fairly constant.

Pelvis: The dorsoventral and mediolateral diameters of the pelvic inlet are fairly constant for the PLSmax and PLSmin pelves (Fig. 2.4B). In the PLSmax (small) pelvis, the inferior pubic ramus is more anteriorly positioned relative to the superior pubic ramus such that the birth canal is relatively wide in the PLSmax (small) pelvis. The ischium spreads laterally such that the bi-ischial distance is greater relative to the overall size at the outlet in the PLSmax (small) pelvis. Furthermore, the sacrum projects more posteriorly in the PLSmax (small) pelvis. Collectively, the birth canal is large relative to the overall size of the pelvis at both the pelvic inlet and outlet in the PLSmax (small) pelvis (Fig. 2.4B; see SI, Fig. S2.8 for measurements of diameters of the pelvic inlet and outlet relative to overall pelvic size).

Discussion

Results of the in-silico simulation show that the fetal head should change its orientation such that the face of the fetus is oriented toward the caudal direction rather than to the pubic direction of the mother to ease childbirth (Fig. 2.1, SI, Figs. S2.4, S2.5). Thus, head rotation is required for the fetus to pass through the birth canal with less obstruction in rhesus macaques. This is consistent with a field observation of childbirth in black macaques (*M. nigra*) (Duboscq et al., 2008). Our results are also consistent with findings of Stoller's pioneering study (Stoller, 1996) in two respects: The first is the fetal rotation observed in Stoller's study, with dorsal flexion of the fetal head during childbirth in *Papio* that have longer snouts (Stoller, 1996). Our data add further evidence to the notion that fetal rotation during childbirth is required not only in primates with long snouts, but also in those with relatively short snouts (rhesus macaques). The second is fetal neck extension. Orienting the face toward the caudal direction of the mother should require neck extension of the fetus. This is consistent with Stoller's finding that neck extension is a way to alleviate obstructed labor in non-human primates with high cephalopelvic proportions (Stoller, 1996). While these inferences could be drawn from our data, there are two factors that remain to be elucidated, one each on the fetal and maternal side. The first is the temporary deformation of the fetal head. In our sample, ten out of twelve fetuses exhibit unfused metopic sutures (with varying degree of fusion; SI, Fig. S2.2). The unfused metopic suture permits the temporary deformation of the fetal skull (Falk et al., 2012). Given the narrow width of the pelvic outlet relative to the fetal skull width (SI, Fig. S2.4, Table S2.4), it is likely that some degree of deformation occurs when the fetus passes through the pelvic outlet. The second is the ligamentary relaxation of the maternal pelvis. The varying degree of the fusion/closure of the metopic suture suggests varying degree of skull deformation. In cases when the degree of skull deformation during delivary is low, it is the pelvis that should remodel to widen the birth canal (Laudicina & Cartmill, 2019). Stoller also reported the effect of ligamentary relaxation (Stoller, 1996). With the CT-based data for static condition obtained in this study, direct evaluation of these factors are difficult. Further evaluation by means of real time tracking of the delivery processes (Ami et al., 2019) is needed to reveal the actual processes of childbirth in rhesus macaques.

The analyses of the three-dimensional morphologies show that the forms of the fetal skull and maternal pelvis exhibit a relatively high level of covariation (supporting H0), and that the CPC along PLS1 axes is largely explained by the covariation of the fetal skull and birth canal (Figs. 2.3, 2.4; supporing H1). Furthermore, the direction of the morphological variation is consistent (i.e., along the mediolateral direction) in the fetal skull and maternal pelvis (Fig. 2.4). The morphological features found in the small-sized (PLSmax) pelvis are consistent with female-

specific features of the pelvis that were previously reported in macaques, such as the large dorsoventral diameter of the pelvic inlet and width of the pelvic inlet and outlet (Moffett, 2017). This indicates that female-specific features are expressed in the small-sized pelvis to a greater extent. Thus, our data show that the pattern of CPC reduces the risk of obstructed labor, which supports H2.

Collectively, our data provide strong support for the hypothesis that the fetal skull and maternal pelvis exhibit the morphological covariation in order to reduce the risk of obstructed labor in rhesus macaques. The fetal skull and maternal pelvis, however, show some features that do not follow expectations under H1 (CPC to ease childbirth). First, not all the birth canal-related locations contribute to CPC. Specifically, the PLSC scores were relatively low at the acetabulum and sacroiliac joints (Fig. 2.3), even though they are relevant components of the birth canal. Furthermore, the morphological variance was relatively low at these locations (SI, Fig. S2.9). We hypothesize that CPC-related plasticity is constrained in these locations since they are also relevant for locomotor function. Increasing bi-acetabular distance and width of the sacrum would cause an increased width of the trunk owing to its morphological covariation with the pelvis (Torres-Tamayo et al., 2018), which could result in increased body weight and reduced locomotor efficiency. Furthermore, an increased bi-acetabular distance could hamper arboreal locomotor behaviors (Badoux, 1974). These inferences are in accordance with the framework of "obstetric dilemma" for pelvic morphology and bipedal locomotion in humans (Rosenberg, 1992; Rosenberg & Trevathan, 1995; Ruff, 1995; Wittman & Wall, 2007) [but see Dunsworth et al. (2012); Warrener et al. (2015)]. Second, the mediolateral diameter of the fetal skull is constant for small and large skulls (Fig. 2.4) even though the constant diameter of the fetal skull can contribute to obstructed labor. We hypothesize that the maintenance of a certain diameter of the cranium is relevant for keeping a certain size and shape of the brain during early ontogeny. It has been suggested that the spatial relationship of the craniofacial complex, i.e., basic craniofacial shape, is already established by the fetal period [macaques (J. E. Sirianni & Newell-Morris, 1980; Joyce E Sirianni & Swindler, 1985); humans (Burdi, 1969; Houpt, 1970; Lavelle, 1974; Trenouth, 1985)]. It is thus likely that the large mediolateral diameter of the skull during the fetal period is a developmental requisite. These hypotheses on functional and developmental constraints on the maternal pelvis and the fetal skull should be further tested.

Our data show that the CPC is present in a primate taxon that does not exhibit a specialized locomotor behavior such as obligate bipedality nor extreme encephalization as modern humans. It appears the pattern of covariation observed in rhesus macaques is at least partly similar to that in humans. For example, the sacrum is more posteriorly projected in the

small-sized pelvis in rhesus macaques (Fig. 2.4B) as observed in human females with short stature (Fischer & Mitteroecker, 2015). On the other hand, the shape of the pelvic inlet is fairly similar in small- and large-sized pelves in rhesus macaques (Fig. 2.4B) while it differs between human females with short and tall stature (Fischer & Mitteroecker, 2015). It is likely that different patterns of the CPC in humans and rhesus macaques reflect different patterns of obstetric constraint. Our data indicate that the CPC could evolve in different ways in each primate taxa reflecting taxon-specific patterns of obstetric difficulty and locomotor constraint.

The mechanisms behind the observed CPC remain to be elucidated. Fischer and Mitteroecker (2015) proposed a correlational selection on the morphologies of the skull and pelvis via genetic linkage due to their proximity in chromosomes and pleiotropic effects of one locus or multiple loci that are unlinked with each other. Our data suggest that such mechanisms at the genetic level could be shared in humans and rhesus macaques. Further studies on genotype-phenotype correlations, from the perspective that the mechanisms of CPC could be shared in humans and macaques, are required to answer these questions.

The limited sample size of the present study must be considered in the interpretation of the results, and a detailed evaluation of the questions raised here must await further studies. However, our data showing that the CPC is not unique to humans have broad implications for the study of evolution of childbirth in primates. We have shown that rhesus macaques, which have neither obligate bipedal locomotion nor extreme encephalization as modern humans, exhibit the CPC. This indicates that specialized pelvic morphology and a high degree of encephalization are not necessarily required for the acquisition of the CPC, and that the CPC can be more generalized than previously thought. There could be two scenarios for evolution of the CPC that remain to be tested. The first scenario is that the CPC evolved independently in humans and macaques, and possibly in other primates such as New World monkeys (NWMs) with high cephalopelvic proportions. The alternative scenario is that the CPC evolved in the early catarrhines before the split of the Hominoidea and Cercopithecoidea, or even prior to the divergence of stem catarrhines given high degree of cephalopelvic proportions in some NWMs. The latter scenario indicates that the CPC evolved prior to the acquisition of bipedal locomotion and encephalization in the human lineage and may in fact be an anthropoid synapomorphy. These scenarios remain to be tested with a larger sample of primates, especially including taxa with low cephalopelvic proportions such as great apes. The evaluation of a wider range of primate taxa in future studies is of special relevance to clarify the CPC-perspective in the morphological evolution of the skull and pelvis.

References

Ami, O., Maran, J. C., Gabor, P., Whitacre, E. B., Musset, D., Dubray, C., Mage, G., & Boyer, L. (2019). Three-dimensional magnetic resonance imaging of fetal head molding and brain shape changes during the second stage of labor. *PLOS ONE, 14*(5).

Badoux, D. M. (1974). An introduction to biomechanical principles in primate locomotion and structure. *Primate locomotion*.

Berge, C., Orban-Segebarth, R., & Schmid, P. (1984). Obstetrical interpretation of the australopithecine pelvic cavity. *Journal of Human Evolution, 13*(7), 573-587. doi:https://doi.org/10.1016/S0047-2484(84)80029-9

Bookstein, F. L. (1991). Morphometric tools for landmark data: Geometry and biology. In: Cambridge: Cambridge University Press.

Burdi, A. R. (1969). Cephalometric growth analyses of the human upper face region during the last two trimesters of gestation. *American Journal of Anatomy, 125*(1), 113-122. doi:https://doi.org/10.1002/aja.1001250106

Correia, H., Balseiro, S., & De Areia, M. (2005). Sexual dimorphism in the human pelvis: Testing a new hypothesis. *HOMO, 56*(2), 153-160. doi:https://doi.org/10.1016/j.jchb.2005.05.003

DeSilva, J. M. (2011). A shift toward birthing relatively large infants early in human evolution. *Proceedings of the National Academy of Sciences, 108*(3), 1022-1027. doi:10.1073/pnas.1003865108

DeSilva, J. M., & Lesnik, J. J. (2008). Brain size at birth throughout human evolution: A new method for estimating neonatal brain size in hominins. *Journal of Human Evolution, 55*(6), 1064-1074. doi:https://doi.org/10.1016/j.jhevol.2008.07.008

Duboscq, J., Neumann, C., Perwitasari-Farajallah, D., & Engelhardt, A. (2008). Daytime birth of a baby crested black macaque (*Macaca nigra*) in the wild. *Behavioural Processes, 79*(1), 81-84. doi:https://doi.org/10.1016/j.beproc.2008.04.010

Dunsworth, H. M., Warrener, A. G., Deacon, T., Ellison, P. T., & Pontzer, H. (2012). Metabolic hypothesis for human altriciality. *Proceedings of the National Academy of Sciences, 109*(38), 15212-15216. doi:10.1073/pnas.1205282109

Escoufier, Y. (1973). Le traitement des variables vectorielles. *Biometrics, 29*(4), 751-760. doi:10.2307/2529140

Falk, D., Zollikofer, C. P. E., Morimoto, N., & Ponce de León, M. S. (2012). Metopic suture of Taung (*Australopithecus africanus*) and its implications for hominin brain evolution. *Proceedings of the National Academy of Sciences, 109*(22), 8467-8470. doi:10.1073/pnas.1119752109

Fischer, B., & Mitteroecker, P. (2015). Covariation between human pelvis shape, stature, and head size alleviates the obstetric dilemma. *Proceedings of the National Academy of Sciences, 112*(18), 5655-5660. doi:10.1073/pnas.1420325112

Foley, R. A., Lee, P. C., Widdowson, E. M., Knight, C. D., Jonxis, J. H. P., Widdowson, E. M., Whiten, A., & Bone, Q. (1991). Ecology and energetics of encephalization in hominid evolution. *Philosophical Transactions of the Royal Society of London. Series B: Biological Sciences, 334*(1270), 223-232. doi:doi:10.1098/rstb.1991.0111

Gibson, K. R. (2002). Evolution of human intelligence: The roles of brain size and mental construction. *Brain, Behavior and Evolution, 59*(1-2), 10-20. doi:10.1159/000063730

Gilmore, J. H., Schmitt, J. E., Knickmeyer, R. C., Smith, J. K., Lin, W., Styner, M., Gerig, G., & Neale, M. C. (2010). Genetic and environmental contributions to neonatal brain structure: A twin study. *Human Brain Mapping, 31*(8), 1174-1182. doi:10.1002/hbm.20926

Hirata, S., Fuwa, K., Sugama, K., Kusunoki, K., & Takeshita, H. (2011). Mechanism of birth in chimpanzees: humans are not unique among primates. *Biology Letters, 7*(5), 686-688. doi:10.1098/rsbl.2011.0214

Houpt, M. I. (1970). Growth of the craniofacial complex of the human fetus. *American Journal of Orthodontics, 58*(4), 373-383. doi:https://doi.org/10.1016/0002-9416(70)90108-9

Huseynov, A., Zollikofer, C. P. E., Coudyzer, W., Gascho, D., Kellenberger, C., Hinzpeter, R., & Ponce de León, M. S. (2016). Developmental evidence for obstetric adaptation of the human female pelvis. *Proceedings of the National Academy of Sciences, 113*(19), 5227-5232. doi:10.1073/pnas.1517085113

Klingenberg, C. P. (2009). Morphometric integration and modularity in configurations of landmarks: tools for evaluating a priori hypotheses. *Evolution & Development, 11*(4), 405-421. doi:10.1111/j.1525-142X.2009.00347.x

Krogman, W. M. (1951). The problem of "timing" in facial growth, with special reference to the period of the changing dentition. *American Journal of Orthodontics, 37*(4), 253-276. doi:https://doi.org/10.1016/0002-9416(51)90086-3

Laudicina, N. M., & Cartmill, M. (2019). *Obstetric constraints in large-brained cebids and modern humans: A comparison of coping mechanisms.* Paper presented at the American Journal of Physical Anthropology.

Lavelle, C. (1974). An analysis of foetal craniofacial growth. *Annals of human biology, 1*(3), 269-287.

Leutenegger, W. (1974). Functional aspects of pelvic morphology in simian primates. *Journal of Human Evolution, 3*(3), 207-222. doi:https://doi.org/10.1016/0047-2484(74)90179-1

Leutenegger, W. (1982). Encephalization and obstetrics in primates with particular reference to human evolution. In *Primate brain evolution* (pp. 85-95). Boston: Springer.

Lovejoy, C. O. (2005). The natural history of human gait and posture: Part 1. Spine and pelvis. *Gait & Posture, 21*(1), 95-112. doi:https://doi.org/10.1016/j.gaitpost.2004.01.001

Moffett, E. A. (2017). Dimorphism in the size and shape of the birth canal across anthropoid primates. *The Anatomical Record, 300*(5), 870-889. doi:10.1002/ar.23572

Morimoto, N., Ogihara, N., Katayama, K., & Shiota, K. (2008). Three-dimensional ontogenetic shape changes in the human cranium during the fetal period. *Journal of Anatomy, 212*(5), 627-635. doi:10.1111/j.1469-7580.2008.00884.x

Primate Research Institute, K. U. (2010). Guide for the care and use of laboratory primates. In (3rd ed.): Primate Research Institute, Kyoto University Inuyama, Japan.

Roberts, A. M., & Thorpe, S. K. S. (2014). Challenges to human uniqueness: bipedalism, birth and brains. *Journal of Zoology, 292*(4), 281-289. doi:10.1111/jzo.12112

Rohlf, F. J., & Corti, M. (2000). Use of two-block partial least-squares to study covariation in shape. *Systematic Biology, 49*(4), 740-753. doi:10.1080/106351500750049806

Rosenberg, K. (1992). The evolution of modern human childbirth. *American Journal of Physical Anthropology, 35*(S15), 89-124. doi:10.1002/ajpa.1330350605

Rosenberg, K., & Trevathan, W. (1995). Bipedalism and human birth: The obstetrical dilemma

revisited. *Evolutionary Anthropology: Issues, News, and Reviews, 4*(5), 161-168. doi:10.1002/evan.1360040506

Rosenberg, K., & Trevathan, W. (2002). Birth, obstetrics and human evolution. *BJOG: An International Journal of Obstetrics & Gynaecology, 109*(11), 1199-1206. doi:10.1046/j.1471-0528.2002.00010.x

Ruff, C. B. (1995). Biomechanics of the hip and birth in early *Homo*. *American Journal of Physical Anthropology, 98*(4), 527-574. doi:10.1002/ajpa.1330980412

Schultz, A. H. (1949). Sex differences in the pelves of primates. *American Journal of Physical Anthropology, 7*(3), 401-424. doi:10.1002/ajpa.1330070307

Schultz, A. H. (1969). *The life of primates*. New York: Universe Books.

Sirianni, J. E., & Newell-Morris, L. (1980). Craniofacial growth of fetal *Macaca nemestrina*: A cephalometric roentgenographic study. *American Journal of Physical Anthropology, 53*(3), 407-421. doi:10.1002/ajpa.1330530312

Sirianni, J. E., & Swindler, D. R. (1985). *Growth and development of the pigtailed macaque*: CRC Press.

Smit, D. J. A., Luciano, M., Bartels, M., van Beijsterveldt, C. E. M., Wright, M. J., Hansell, N. K., Brunner, H. G., Estourgie-van Burk, G. F., de Geus, E. J. C., Martin, N. G., & Boomsma, D. I. (2010). Heritability of head size in Dutch and Australian twin families at ages 0–50 years. *Twin Research and Human Genetics, 13*(4), 370-380. doi:10.1375/twin.13.4.370

Stoller, M. K. (1996). The obstetric pelvis and mechanism of labor in nonhuman primates.

Sze, E. H. M., Kohli, N., Miklos, J. R., Roat, T., & Karram, M. M. (1999). Computed tomography comparison of bony pelvis dimensions between women with and without genital prolapse. *Obstetrics & Gynecology, 93*(2), 229-232. doi:https://doi.org/10.1016/S0029-7844(98)00376-7

Tague, R. G. (1991). Commonalities in dimorphism and variability in the anthropoid pelvis, with implications for the fossil record. *Journal of Human Evolution, 21*(3), 153-176. doi:https://doi.org/10.1016/0047-2484(91)90059-5

Tague, R. G., & Lovejoy, C. O. (1986). The obstetric pelvis of A.L. 288-1 (Lucy). *Journal of*

Human Evolution, 15(4), 237-255. doi:https://doi.org/10.1016/S0047-2484(86)80052-5

Torres-Tamayo, N., García-Martínez, D., Nalla, S., Barash, A., Williams, S. A., Blanco-Pérez, E., Mata Escolano, F., Sanchis-Gimeno, J. A., & Bastir, M. (2018). The torso integration hypothesis revisited in *Homo sapiens*: Contributions to the understanding of hominin body shape evolution. *American Journal of Physical Anthropology, 167*(4), 777-790. doi:10.1002/ajpa.23705

Trenouth, M. J. (1985). The relationship between differences in regional growth rates and changes in shape during human fetal craniofacial growth. *Archives of Oral Biology, 30*(1), 31-35. doi:https://doi.org/10.1016/0003-9969(85)90021-4

Trevathan, W. R. (1988). Fetal emergence patterns in evolutionary perspective. *American Anthropologist, 90*(3), 674-681. doi:10.1525/aa.1988.90.3.02a00100

Trevathan, W. R. (2015). Primate pelvic anatomy and implications for birth. *Philosophical Transactions of the Royal Society B: Biological Sciences, 370*(1663), 20140065. doi:10.1098/rstb.2014.0065

Trevathan, W. R. (2017). *Human birth: An evolutionary perspective*: Routledge.

Warrener, A. G., Lewton, K. L., Pontzer, H., & Lieberman, D. E. (2015). A wider pelvis does not increase locomotor cost in humans, with implications for the evolution of childbirth. *PLOS ONE, 10*(3), e0118903. doi:10.1371/journal.pone.0118903

Washburn, S. L. (1942). Skeletal proportions of adult langurs and macaques. *Human biology, 14*(4), 444.

Washburn, S. L. (1960). Tools and human evolution. *Scientific American, 203*(3), 62-75.

Wells, J. C. K., DeSilva, J. M., & Stock, J. T. (2012). The obstetric dilemma: An ancient game of Russian roulette, or a variable dilemma sensitive to ecology? *American Journal of Physical Anthropology, 149*(S55), 40-71. doi:10.1002/ajpa.22160

Wittman, A. B., & Wall, L. L. (2007). The evolutionary origins of obstructed labor: Bipedalism, encephalization, and the human obstetric dilemma. *Obstetrical & Gynecological Survey, 62*(11), 739-748. doi:10.1097/01.ogx.0000286584.04310.5c

Zelditch, M. L., Swiderski, D. L., & Sheets, H. D. (2012). *Geometric morphometrics for biologists: a primer*: Academic Press.

Zollikofer, C. P. E., & León, M. S. P. d. (2002). Visualizing patterns of craniofacial shape variation in *Homo sapiens*. *Proceedings of the Royal Society of London. Series B: Biological Sciences, 269*(1493), 801-807. doi:doi:10.1098/rspb.2002.1960

Zollikofer, C. P. E., Scherrer, M., & Ponce de León, M. S. (2017). Development of pelvic sexual dimorphism in Hylobatids: Testing the obstetric constraints hypothesis. *The Anatomical Record, 300*(5), 859-869. doi:10.1002/ar.23556

Figures

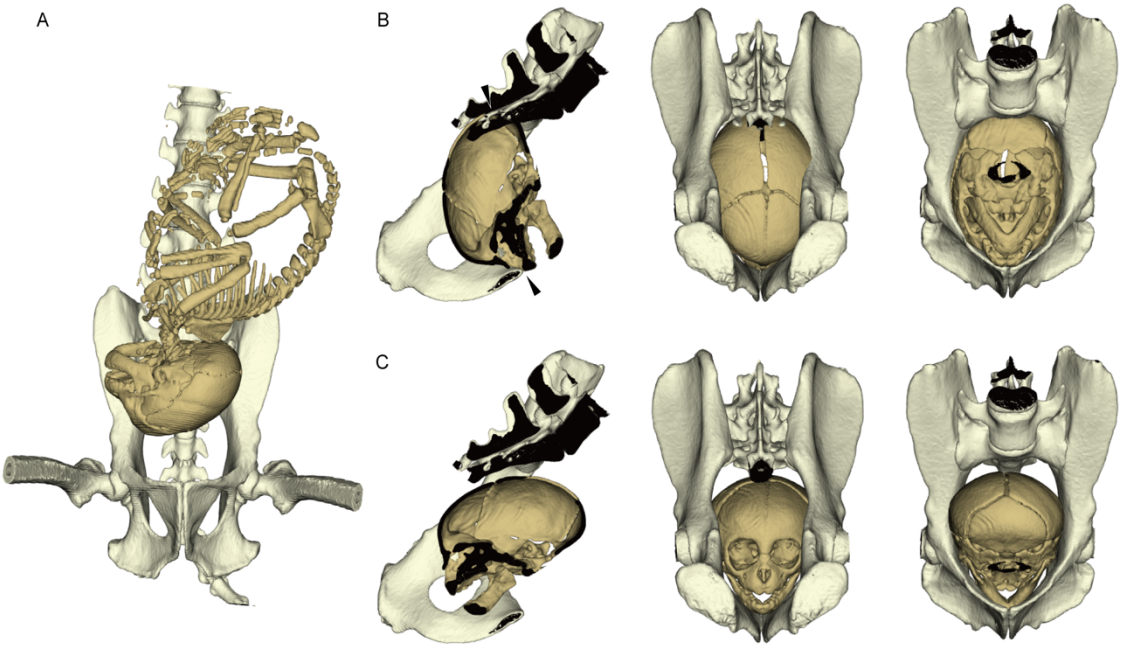

Fig. 2.1 *A*: CT-based rendering of the perinatal fetal skeleton and maternal pelvis of rhesus macaques [IDs: PRI-Mm1752 (mother) and PRI-Mm2059 (fetus)]. *B*, *C*: the *in-silico* simulation of the childbirth with the fetal head facing toward the pubic (*B*) and caudal (*C*) directions of the mother [midsagittal section (left), caudal view (middle), and superior view (right)]. The cephalopelvic proportion is higher at the pelvic outlet than at the pelvic inlet. B: black arrowheads indicate "crash points" where the fetal head exceeds the dimensions of the maternal birth canal. *C*: fetuses that face the caudal direction of the mother result in a lessened risk of obstruction since the anteroposterior diameter of the head is larger than that of the pelvic inlet. Note that the mediolateral diameter of the fetal head is considerably larger than that of the pelvic outlet of the maternal birth canal. See *SI*, Figs. S2.1, S2.4, S2.5 for the simulation of other dyads

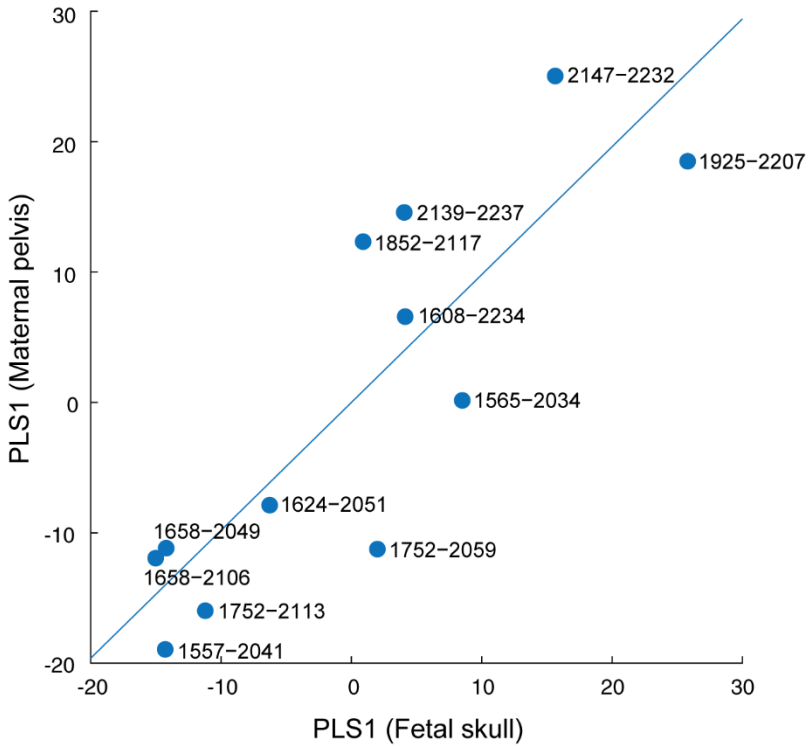

Fig. 2.2 Plot graph of the PLS1 scores of the fetal skull and maternal pelvis. Numbers indicate IDs of mothers and fetuses (PRI-Mm-numbers).

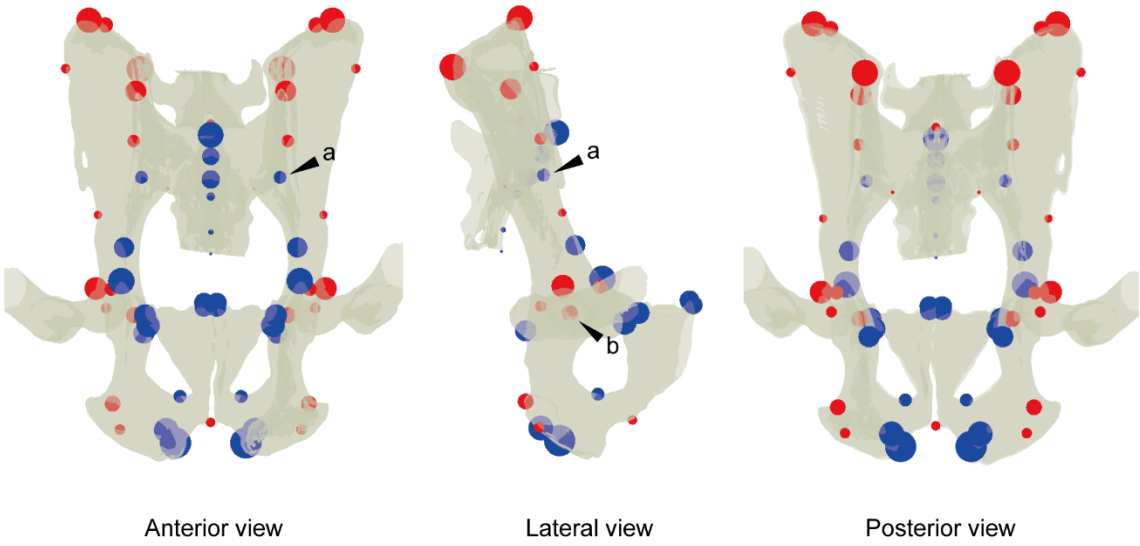

Fig. 2.3 Visualization of the PLSC scores. The proportion of the PLS1-related variation to total variation is visualized as different sized spheres [blue: birth canal-related landmarks (see Materials and Methods and *SI*, Table S2.3 for definition), red: other locations]. The PLSC score is generally high at birth canal-related locations (with exceptions such as the location indicated by the arrowhead 'a'). Conversely, the PLSC score is generally low at locomotion-related locations [e.g., at the acetabulum (indicated by the arrowhead 'b')].

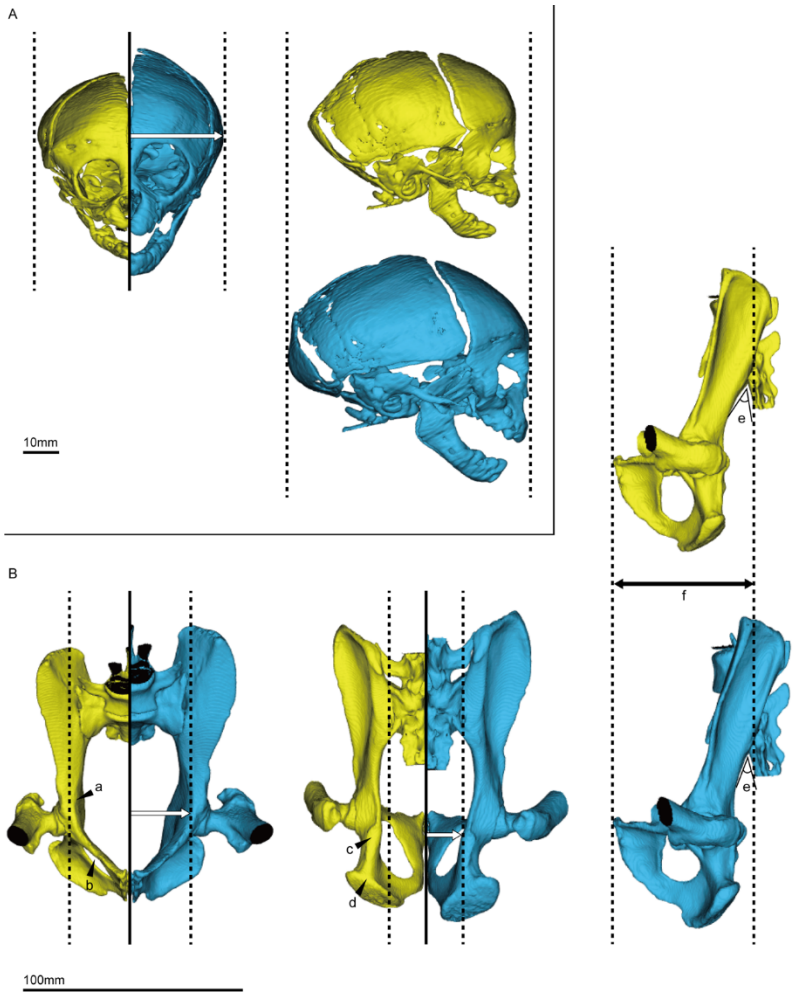

Fig. 2.4 Morphological variations of the fetal skull (*A*) and maternal pelvis (*B*) along PLS1 axes. The yellow and blue models correspond to PLSmax (small) and PLSmin (large), respectively. The width of the fetal skull and the pelvic inlet remain fairly constant despite the differences of the overall sizes [leftmost panels in *A* (fetal skull) and *B* (maternal pelvis); dotted lines and arrows show the width defined in the blue model]. *B*: the small-sized pelvis (yellow) has larger birth canal dimensions relative to the whole pelvic size than the large-sized pelvis (blue). The markers (a–f) indicate features of the small-sized pelvis (yellow) compared to the large-sized pelvis (blue). The arrowhead 'a' indicates the relative expansion of the width of the pelvic inlet. The arrowhead 'b' indicates the inferior pubic ramus is more anteriorly positioned relative to the superior pubic ramus such that the pelvic outlet is relatively large (expressed also as visibility of the *foramen obturatum* in this view). The arrowheads 'c' and 'd' indicate the relative expansion of the pelvic outlet at the ischial spines (c) and ischial tuberosities (d). The angle between the *os coxa* and sacrum is greater (e), which results in the relative expansion of the dorsoventral dimeter of the birth canal (f).

Supporting Information

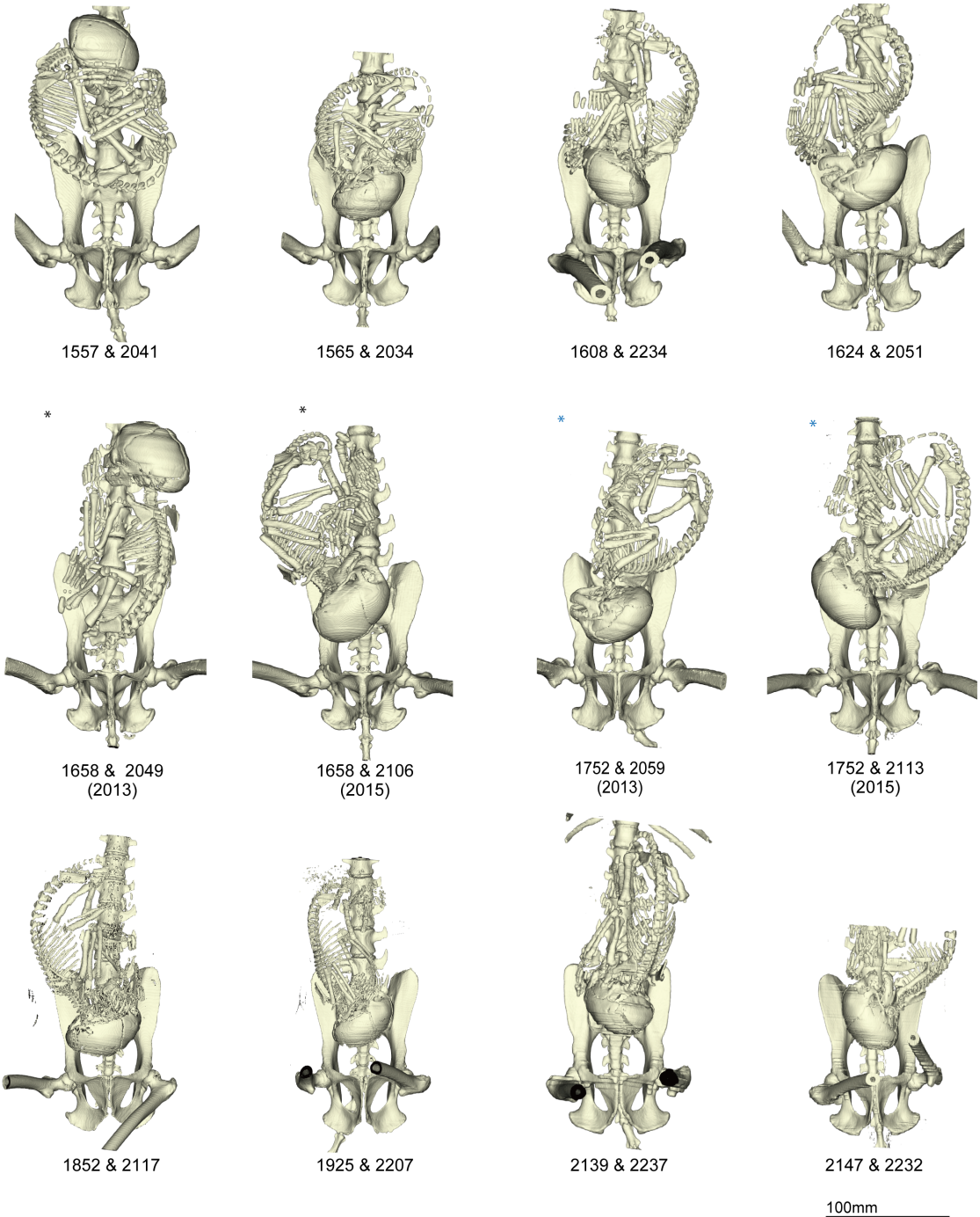

Fig. S2.1 The sample of mother−fetus dyads of the rhesus macaques used in this study (medical computed tomography-based rendering of the fetal skeleton and maternal pelvis during the perinatal period). Numbers indicate IDs of mothers and fetuses (PRI-Mm-numbers). The asterisks indicate the same mothers in different years.

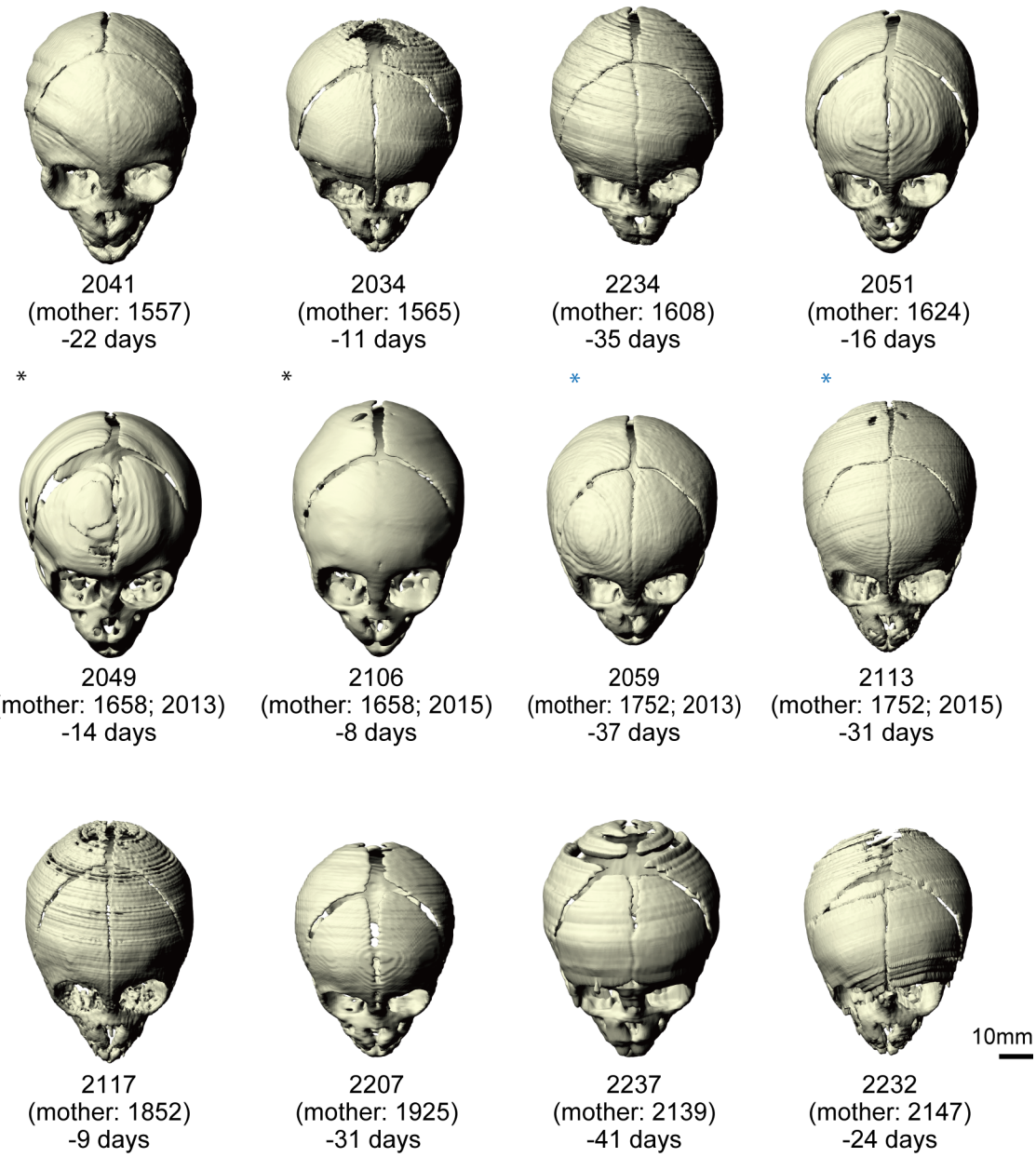

Fig. S2.2 The fetal skulls of the rhesus macaques used in this study. In our sample, ten out of twelve fetuses exhibit unfused metopic sutures (with varying degree of fusion/closure). Days indicate the time lags between dates of the birth and CT scan. Numbers indicate IDs (PRI-Mm-numbers). The asterisks indicate the fetuses from same mothers in different years.

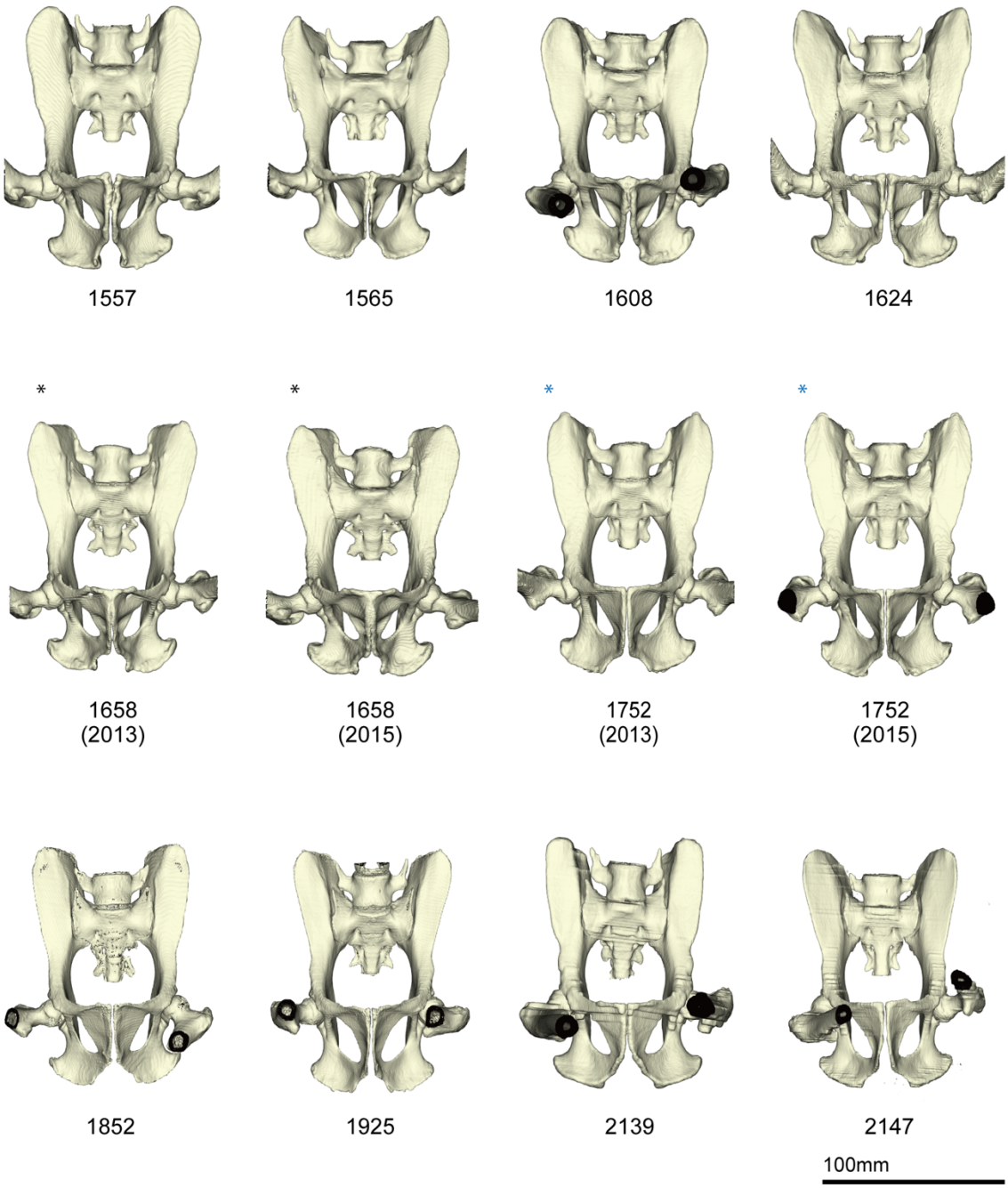

Fig. S2.3 The maternal pelves of the rhesus macaques used in this study. Numbers indicate IDs (PRI-Mm-numbers). The asterisks indicate the same individuals in different years.

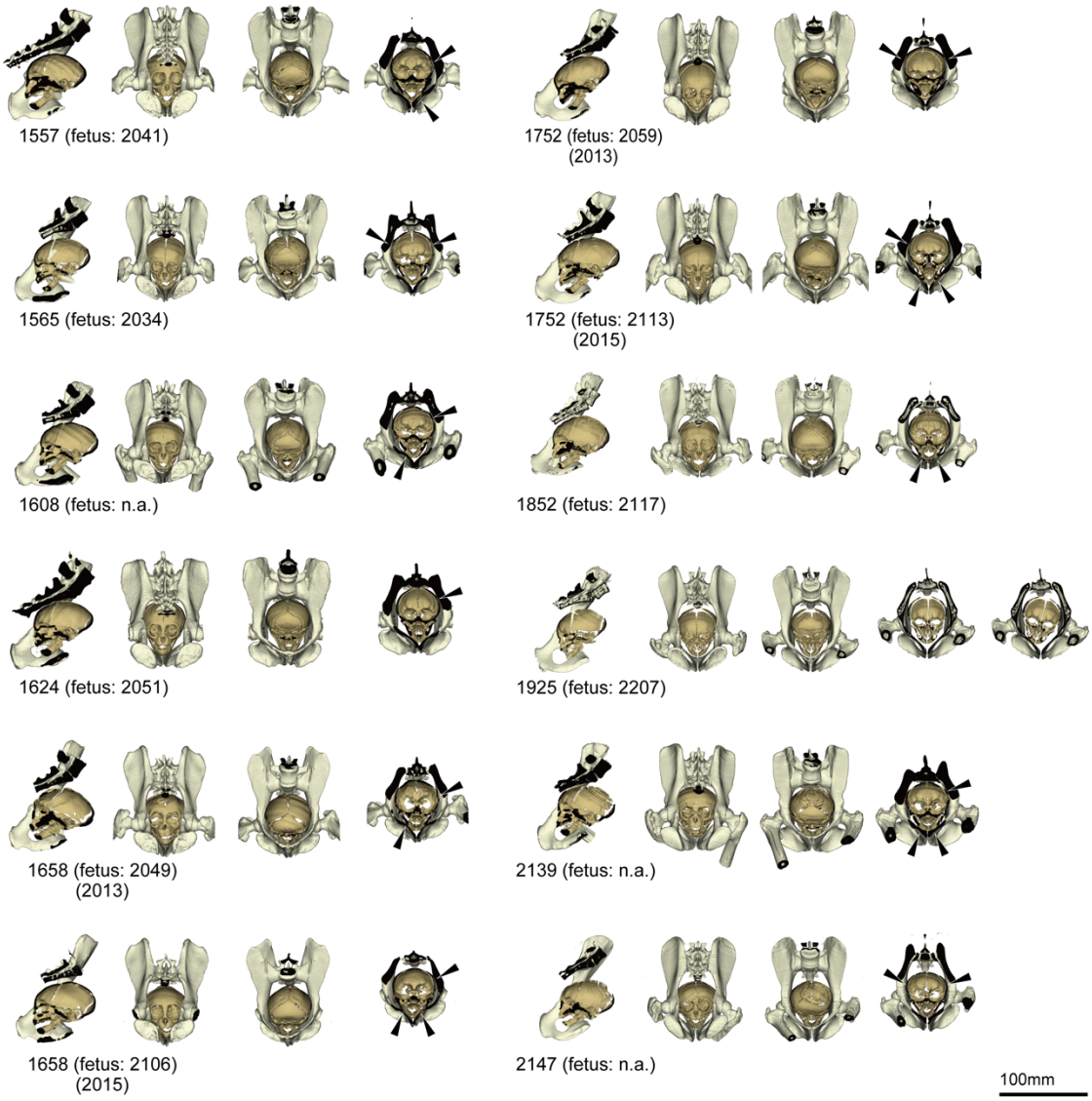

Fig. S2.4 The *in-silico* simulation of the childbirth with the fetal face facing toward the caudal direction of the mother. Left: midsagittal section, second from left: caudal view, third from left: superior view, right: transverse section that goes through the center of first sacral vertebra and pubic symphysis. Black arrowheads indicate “crash points” where the fetal head exceeds the dimensions of the maternal birth canal. The results show that rotation, with which the fetal head is in oblique position relative to the maternal pelvis, is not likely in most dyads (eleven out of twelve). Numbers indicate IDs of mothers and fetuses (PRI-Mm-numbers).

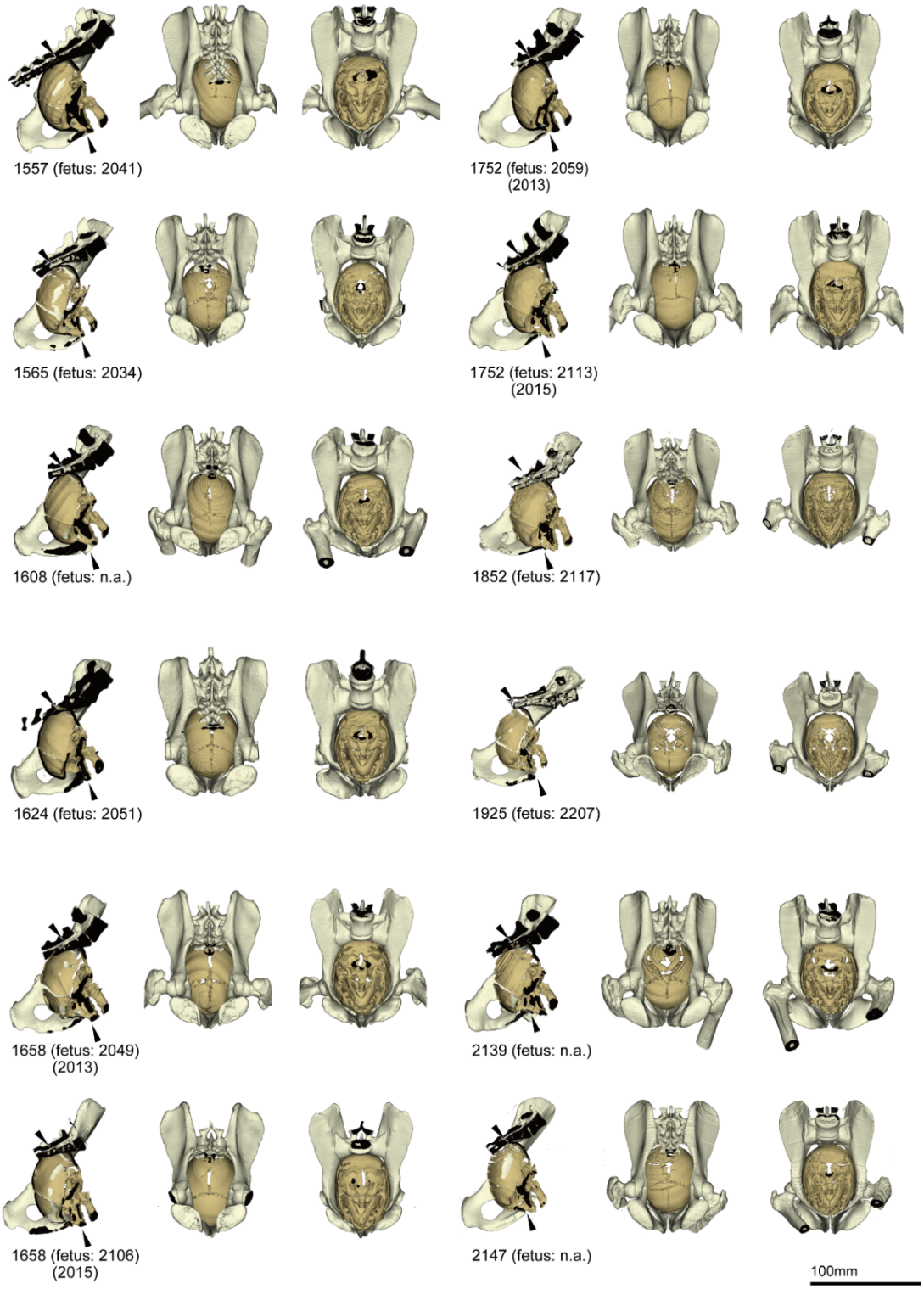

Fig. S2.5 The *in-silico* simulation of the childbirth with the fetal face facing toward the pubic direction of the mother. Left: midsagittal section, middle: caudal view, right: superior view. Black arrowheads indicate the "crash points" where the fetal head exceeds the dimensions of the maternal birth canal. Numbers indicate IDs of mothers and fetuses (PRI-Mm-numbers).

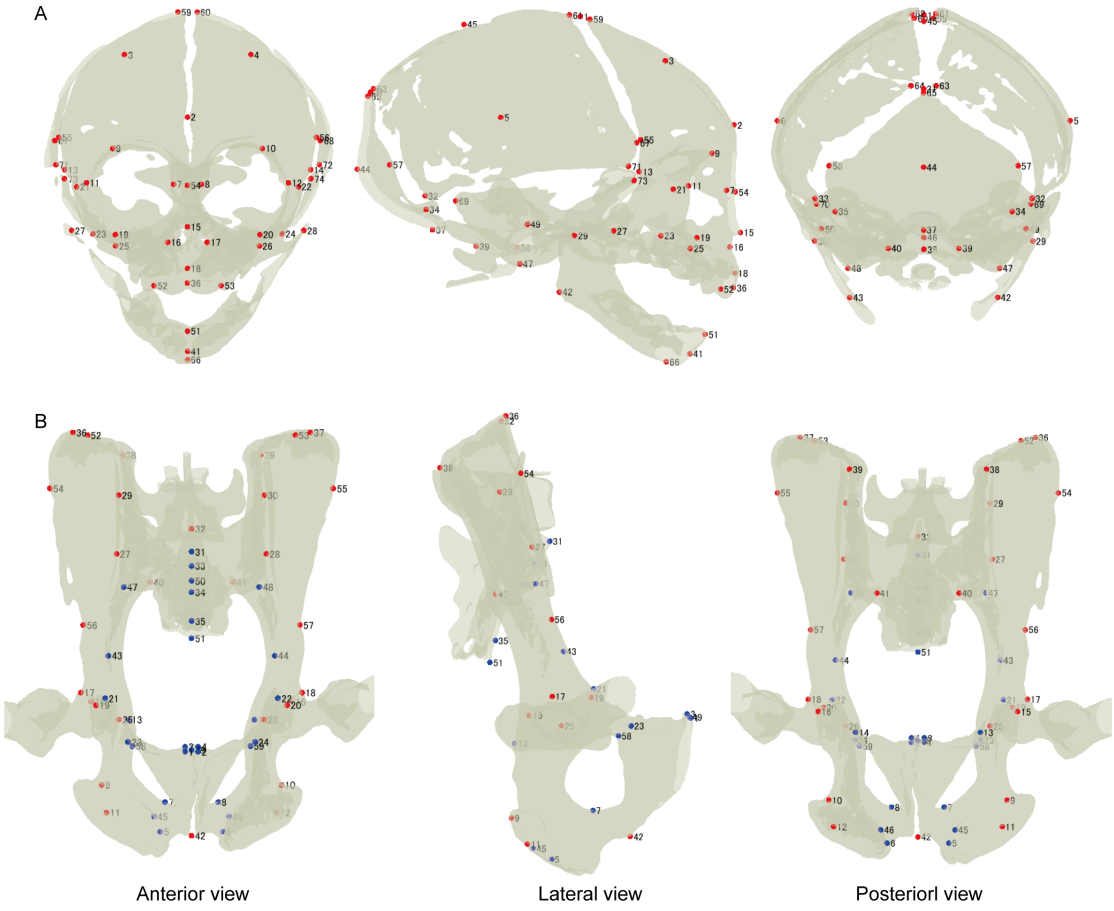

Fig. S2.6 Landmarks used in this study. See Tables S2.2 and S2.3 for definitions. *A*: fetal skull. *B*: maternal pelvis (blue: birth canal-related landmarks, red: other landmarks).

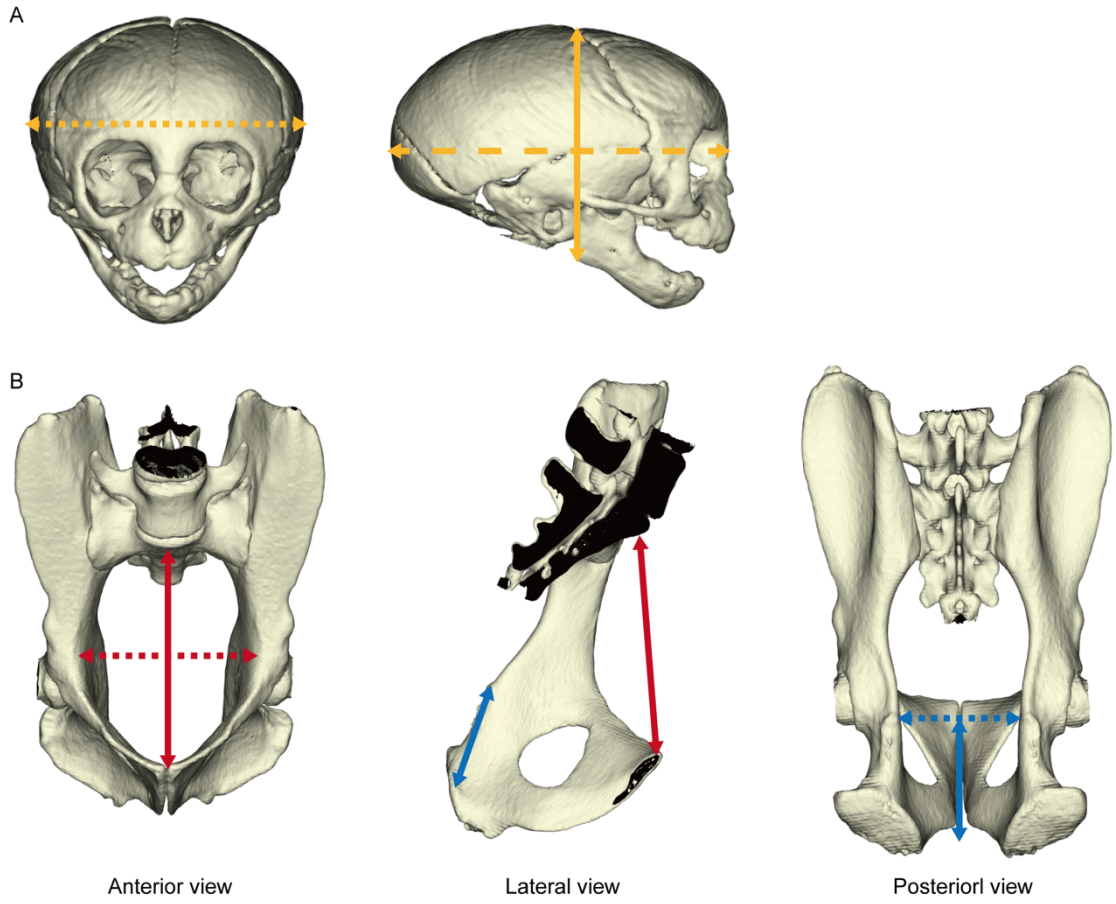

Fig. S2.7 Measurement of diameters. *A*: fetal skull. *B*: maternal pelvis. *A*: the dotted line indicates the mediolateral diameter (skull width: #5–#6 in Table S2.2). The solid line indicates the superoinferior diameter (skull height: from the midpoint of #42 and #43 to #1 in Table S2.2). The broken line indicates the anteroposterior diameter (skull length: #44–#54 in Table S2.2). *B*: the red and blue arrows with solid lines indicate the dorsoventral diameter of the pelvic inlet (#31–#49 in Table S2.3) and outlet (from the midpoint of #13 and #14 to the midpoint of #45 and #46 in Table S2.3), respectively. The red and blue arrows with dotted lines indicate mediolateral diameters of the pelvic inlet (#43–#44 in Table S2.3) and outlet (#13–#14 in Table S2.3), respectively. We referred to descriptions in the literature (Bast et al., 1933; Schultz, 1949) to define the measurements for the pelvic inlet and outlet on the pelvis.

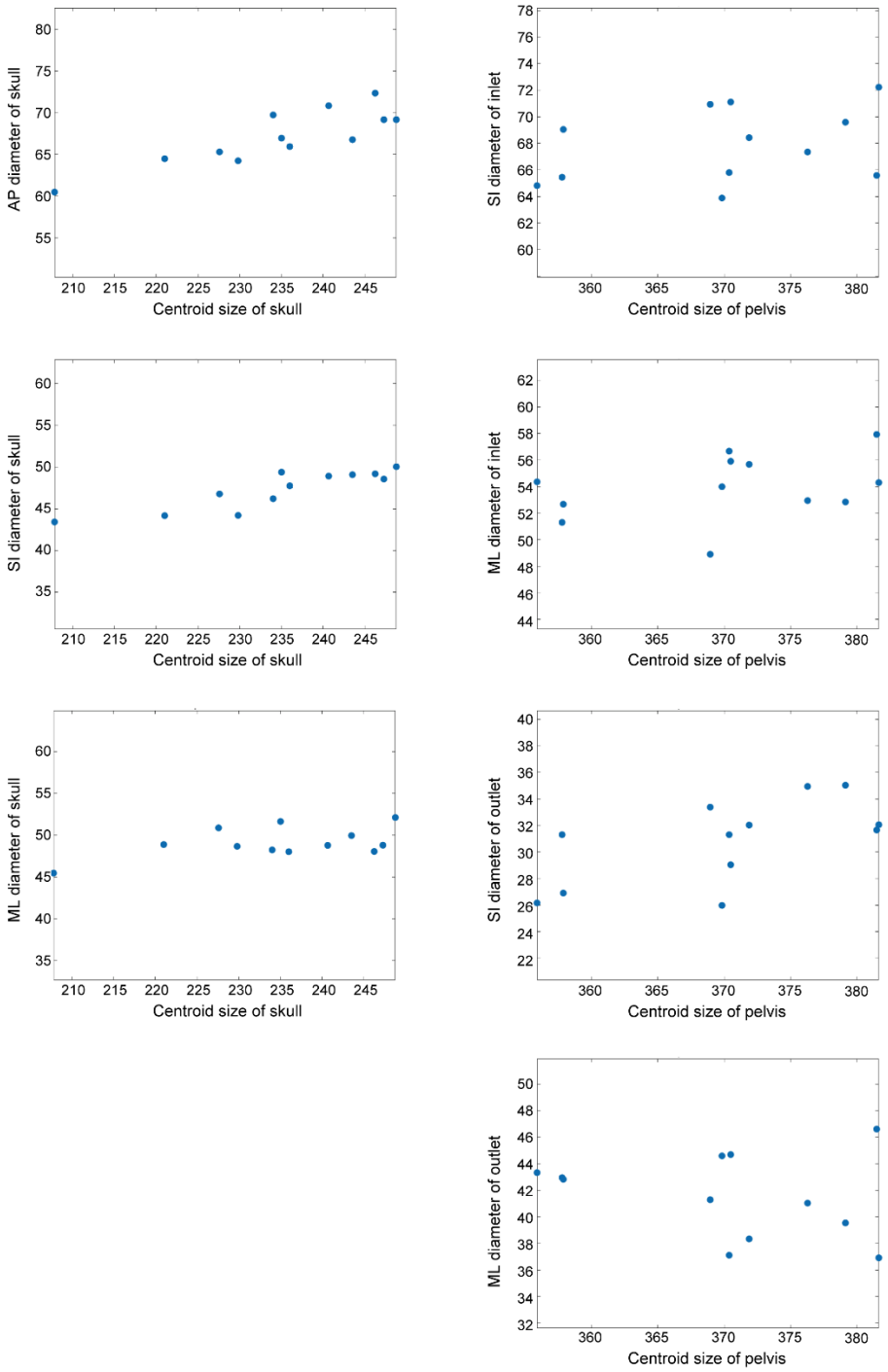

Fig. S2.8 Plot graphs of the centroid sizes and diameters (mm) of the skull/pelvis (skull: left panel, pelvis: right panel). There is a tendency that the width of the skull remains constant independent of the overall size of the skull. Likewise, diameters of the birth canal tend to remain constant independent of the overall size of the pelvis.

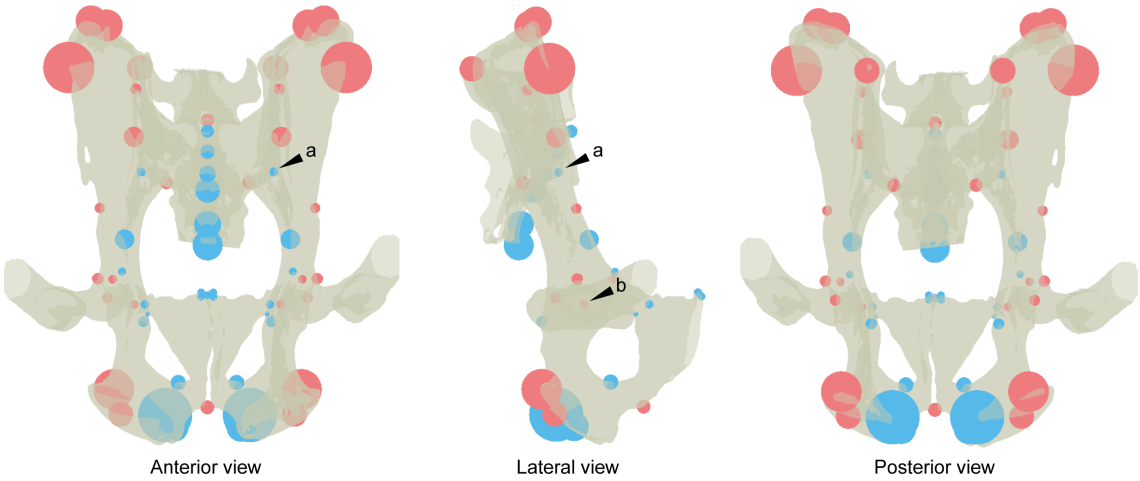

Fig. S2.9 Visualization of the coordinate variation for each landmark. The proportion of the variation is visualized as size differences of spheres [pale blue: birth canal-related landmarks (see methods and Table S2.2 for definition), pink: other locations]. The variation is generally low at locomotion-related locations [*e.g.*, at the sacroiliac joint (indicated by the arrowhead 'a') and acetabulum (indicated by the arrowhead 'b')].

Table S2.1 Sample information.

ID (mothers)	Date of birth (mothers)	Body weight of mothers (kg) (date of measurement)	ID (fetuses)	Date of CT scan	Date of delivery	Days between the birth and CT scan	PRICT ID*
PRI-Mm1557	2000/5/18	10.8 (2013/06/25)	PRI-Mm2041	2013/5/16	2013/6/7	-22	1526
PRI-Mm1565	2000/5/29	5.2 (2013/08/09)	PRI-Mm2034	2013/5/16	2013/5/27	-11	1528
PRI_Mm1608	2001/7/6	6.9 (2019/03/19)	PRI-Mm2234	2020/4/15	2020/5/20	-35	1527
PRI-Mm1624	2002/5/5	9.6 (2013/07/10)	PRI-Mm2051	2013/6/11	2013/6/27	-16	1529
PRI-Mm1658 (2013)	2003/6/13	6.0 (2013/08/27)	PRI-Mm2049	2013/6/11	2013/6/25	-14	1530
PRI-Mm1658 (2015)		8.0 (2015/06/10)	PRI-Mm2106	2015/5/19	2015/5/27	-8	1531
PRI-Mm1752 (2013)	2006/5/8	9.1 (2013/08/09)	PRI-Mm2059	2013/6/11	2013/7/18	-37	1532
PRI-Mm1752 (2015)		8.9 (2015/07/09)	PRI-Mm2113	2015/5/19	2015/6/19	-31	1533
PRI-Mm1852	2008/7/15	5.6 (2015/08/06)	PRI-Mm2117	2015/6/17	2015/6/26	-9	1537
PRI-Mm1925	2010/6/13	6.0 (2018/05/17)	PRI-Mm2207	2018/4/5	2018/5/6	-31	1534
PRI-Mm2139	2016/3/9	5.9 (2019/03/19)	PRI-Mm2237	2020/4/15	2020/5/26	-41	1535
PRI-Mm2147	2016/5/30	3.7 (2019/03/12)	PRI-Mm2232	2020/4/15	2020/5/9	-24	1536

*PRICT ID indicates numbers to identify CT images on the online database, Digital Morphology Museum of KUPRI (http://dmm.pri.kyoto-u.ac.jp/dmm/WebGallery/)

Table S2.2 Definition of the landmarks on the fetal skull.

Landmark numbers	Definition
1	Bregma
2	Glabella
3, 4	Midpoint of #1 and most superior point of supra-orbital margin along shortest path between the two points
5, 6	Eurion
7, 8	Maxillofrontale
9, 10	Most superior point of supra-orbital margin
11, 12	Frontmalare orbitale
13, 14	Sphenion
15	Rhinion
16, 17	Most lateral point of the inferior margin of pirform aperture
18	Akanthion
19 ,20	Orbitale
21, 22	Frontmalare temporale
23, 24	Jugale
25, 26	Most anterior point of zygomatic process of maxilla
27, 28	Mid point of zygomatic process of temporal bone
29, 30	Most posterior point of zygomatic process of temporal bone
31	Lamda
32, 33	Asterion on parietal bone
34, 35	Most antero-lateral point of occipital squama
36	Prosthion
37	Opisthion
38	Basion
39, 40	Most lateral point of foramen magnum
41	Pogonion
42, 43	Gonion
44	Opisthocranion
45	Midpoint between bregma and lamda
46	Sphenobasion
47, 48	Mastoidale
49, 50	Porion
51	Infradentale
52, 53	Inferior point of the margin of premaxilla and maxilla
54	Nasion
55, 56	Sphenion on frontal bone
57, 58	Asterion on occipital bone
59, 60	Most posterior point of frontal bone along the frontal suture
61, 62	Most anterior point of parietal bone along the sagittal suture
63, 64	Most posterior point of parietal bone along the sagittal suture
65	Most superior point of occipital bone
66	Gnathion
67, 68	Sphenion on parietal bone
69, 70	Asterion on temporal bone
71, 72	Krotaphion on parietal bone
73, 74	Krotaphion on temporal bone

Table S2.3 Definition of the landmarks on the maternal pelvis. Numbers with gray background indicate birth canal-related landmarks.

Lundmark numbers	Dentition
1, 2	Most antero-superior point of pubic symphysis
3, 4	Most postero-superior point of pubic symphysis
5, 6	Intersection of ischiopubic junction and medial border of ischial tuberosity
7, 8	Most inferior point of obturator foramen
9, 10	Most postero-superior point of ischial tuberosity
11, 12	Central point of ischial tuberosity
13, 14	Ischial spine
15, 16	Most posterior point of acetabulum
17, 18	Most superior point of acetabulum
19, 20	Superior point of ilio-pubic junction
21, 22	Intersection of arcuate line and ilio-pubic junction
23, 24	Midpoint #1 and #21
25, 26	Deepest point of acetabulum
27, 28	Intersection of arcuate line and sacro-iliac joint
29, 30	Most superior point of sacro-iliac joint
31	Most antero-superior point of S1 (first sacral vertebra)
32	Most postero-superior point of S1
33	Midpoint of anterior side of S1
34	Midpoint of anterior side of S2
35	Midpoint of anterior side of S3
36, 37	Most superior point of iliac spine
38, 39	Most posterior point of iliac crest
40, 41	Most postero-inferior point of iliac spine
42	Most inferior point of pubic symphysis
43, 44	Most lateral part of arcuate line
45, 46	Most interior part of ischial tuberosity
47, 48	Intersection of arcuate line and sacro-iliac joint
49	Most superior point of pubic symphysis
50	Most inferior point of anterior side of S1
51	Most antero-inferior point of sacrum
52, 53	Superior end of arcuate line
54, 55	Most lateral part of iliac ala
56, 57	Lateral margin of the bottom of iliac ala
58, 59	Most superior point of obturator foramen

Table S2.4 Comparison of diameters between the fetal skull and maternal pelvis (birth canal). ML: mediolateral, DV: dorsoventral, SI: superoinferior. See Figs. S2.4 and S2.5 for results of the *in-silico* simulation.

		Maternal pelvis	Fetal skull	Maternal pelvis	Fetal skull	Maternal pelvis	Fetal skull
ID (mothers)	ID (fetuses)	ML diameter of inlet	ML diameter	DV diameter of inlet	SI diameter	DV diameter of inlet	AP diameter
PRI-Mm1557	PRI-Mm2041	54.3	48.1	72.2	49.2	72.2	72.3
PRI-Mm1565	PRI-Mm2034	48.9	50.9	70.9	46.8	70.9	65.3
PRI-Mm1608	PRI-Mm2234	55.9	48.2	71.1	46.2	71.1	69.7
PRI-Mm1624	PRI-Mm2051	57.9	48.8	65.6	48.9	65.6	70.8
PRI-Mm1658 (2013)	PRI-Mm2049	55.7	52.1	68.4	50.0	68.4	69.2
PRI-Mm1658 (2015)	PRI-Mm2106	56.7	48.8	65.8	48.6	65.8	69.2
PRI-Mm1752 (2013)	PRI-Mm2059	52.9	48.7	67.3	44.2	67.3	64.2
PRI-Mm1752 (2015)	PRI-Mm2113	52.8	50.0	69.6	49.1	69.6	66.8
PRI-Mm1852	PRI-Mm2117	54.4	48.0	64.8	47.8	64.8	65.9
PRI-Mm1925	PRI-Mm2207	51.3	45.5	65.4	43.4	65.4	60.5
PRI-Mm2139	PRI-Mm2237	54.0	51.7	63.9	49.4	63.9	66.9
PRI-Mm2147	PRI-Mm2232	52.7	48.9	69.0	44.2	69.0	64.5
		ML diameter of outlet	ML diameter	DV diameter of outlet	SI diameter	DV diameter of outlet	AP diameter
PRI-Mm1557	PRI-Mm2041	36.9	48.1	32.1	49.2	32.1	72.3
PRI-Mm1565	PRI-Mm2034	41.3	50.9	33.4	46.8	33.4	65.3
PRI-Mm1608	PRI-Mm2234	44.7	48.2	29.0	46.2	29.0	69.7
PRI-Mm1624	PRI-Mm2051	46.6	48.8	31.7	48.9	31.7	70.8
PRI-Mm1658 (2013)	PRI-Mm2049	38.3	52.1	32.0	50.0	32.0	69.2
PRI-Mm1658 (2015)	PRI-Mm2106	37.1	48.8	31.3	48.6	31.3	69.2
PRI-Mm1752 (2013)	PRI-Mm2059	41.0	48.7	34.9	44.2	34.9	64.2
PRI-Mm1752 (2015)	PRI-Mm2113	39.5	50.0	35.0	49.1	35.0	66.8
PRI-Mm1852	PRI-Mm2117	43.3	48.0	26.2	47.8	26.2	65.9
PRI-Mm1925	PRI-Mm2207	43.0	45.5	31.3	43.4	31.3	60.5
PRI-Mm2139	PRI-Mm2237	44.6	51.7	26.0	49.4	26.0	66.9
PRI-Mm2147	PRI-Mm2232	42.8	48.9	26.9	44.2	26.9	64.5

References

Bast, T. H., Leonard, S. L., Christensen, K., Lineback, P., Cummins, H., Marshall, J. A., Geist, F. D., Errit S. Miller, J., Hartman, C. G., Miller, R. A., Hines, M., Schultz, A. H., Howell, A. B., Stewart, T. D., Huber, E., William L. Straus, J., Kuntz, A., Sullivan, W. E., & Wislocki, G. B. (1933). *The Anatomy of the rhesus monkey (Macaca mulatta)* (C. G. Hartman & W. L. Straus Eds.). London: The Williams & Wilkins Company.

Schultz, A. H. (1949). Sex differences in the pelves of primates. *American Journal of Physical Anthropology, 7*(3), 401-424. doi:10.1002/ajpa.1330070307

Chapter 3

Human shoulder development is adapted to obstetrical constraints

Published in: *Proceedings of the National Academy of Sciences* 119(16): e2114935119

Introduction

Childbirth is frequently a difficult task for humans compared to other large mammals. The obstetrical difficulties of humans result from a combination of a superoinferiorly short and antero-posteriorly deep pelvis of the mother and a large head and broad shoulders of the neonate. Obstetrical difficulties should, in principle, be eased by expanding the birth canal-related dimensions in the pelvis, especially the sacro–acetabular and biacetabular distances, and/or by reducing the critical cranial and shoulder dimensions of the fetus. However, the high prevalence of obstetrical difficulties in humans indicates that fetopelvic constraints remain unresolved. Various hypotheses have been proposed to explain this pattern. It has been suggested that more expansive pelvic dimensions could reduce the energetic efficiency of bipedal locomotion (Rosenberg, 1992; Rosenberg & Trevathan, 2002; Ruff, 1995; Tague & Lovejoy, 1986; Wittman & Wall, 2007), and that they could also be disadvantageous for bearing the weight of the visceral organs and the fetus during pregnancy (Abitbol, 1988; Brown et al., 2013; Pavličev et al., 2020; Stansfield et al., 2021; Sze et al., 1999), and may increase the risk of knee and ankle injuries due to increased stress along medio-lateral direction (Alentorn-Geli et al., 2009). The resulting obstetrical dilemma (Washburn, 1960) has been hypothesized to persist in modern humans because of opposing and incompatible selective trends favoring large neonatal heads and narrow maternal birth canals (Fischer & Mitteroecker, 2015; Mitteroecker et al., 2016; Pavličev et al., 2020; Stansfield et al., 2021). Recently, the obstetrical dilemma hypothesis was challenged by various studies, indicating that locomotor cost is not increased by wider pelvic dimensions, and proposing that fetal brain growth is constrained by the limits of maternal metabolism rather than by obstetrical constraints (Holly M. Dunsworth et al., 2012).

It has been shown that obstetrical difficulties in humans are eased in various ways on both the maternal and neonatal sides. The first, which relates to mothers, consists in female-specific features of the pelvis, such as the laterally oriented ischiopubic region, flaring iliac blades, wide biacetabular distance, and a posteriorly projected sacrum (Correia et al., 2005; LaVelle, 1995; Moffett, 2017; Rosenberg, 1992; Schultz, 1949). A developmental study showed that these female-specific features are likely related to childbirth since they are expressed most strongly during the reproductive phase (Huseynov et al., 2016). In addition to the female-specific pelvic morphology, hormonal relaxation of the ligaments at the sacroiliac joints and pubic symphysis permits the bony pelvis to temporarily expand the birth canal during late pregnancy and childbirth (BjöRklund et al., 1997; Laudicina & Cartmill, 2019; Stoller, 1996). The second, which relates to both mothers and neonates, is cephalopelvic covariation (Fischer & Mitteroecker, 2015; Chapter 2), which results in corresponding fetal head and maternal pelvic dimensions. The third, which

relates to neonates, is the delayed ossification of the cranial vault during the fetal period. In humans, the fusion of the metopic suture is delayed compared to other primates. The metopic suture of humans is still unfused at birth, which is thought to permit the temporary deformation of the fetal head during childbirth (Ami et al., 2019; Beischer, 1986; Chopra, 1957; Falk et al., 2012). Additionally, the brain mass of the neonate relative to that of adults is smaller in humans (~30%) than in other primates such as chimpanzees (~40%) and macaques (~60%) (DeSilva & Lesnik, 2008). The perinatal head of humans thus shows various developmental features likely associated with amelioration of the obstetrical dilemma and/or optimization of the perinatal metabolic demands of the mother and the fetus (Holly M Dunsworth, 2018; Holly M. Dunsworth et al., 2012).

How then about the broad shoulders of humans? The prevalence of shoulder dystocia, that is the arrest of fetal shoulders in the birth canal, is relatively high in humans (Ouzounian & Gherman, 2005; Øverland et al., 2012). In the contemporary human population, the frequency of shoulder dystocia increases linearly with neonatal body weight (Gherman et al., 2006), and the risk of shoulder dystocia is notably high in the cases of neonatal macrosomia (Bérard et al., 1998; Ezegwui et al., 2011; Ju et al., 2009; Vidarsdottir et al., 2011). The shoulder dystocia can at times cause serious complications: on the fetal/neonatal side, it can cause asphyxia and/or brachial plexus injury that can lead to Erb's palsy (Gross et al., 1987; Sandmire & O'Halloin, 1988; Sjöberg et al., 1988). On the maternal side, it can lead to uterine rupture and/or excessive bleeding and, in the worst case, result in death of neonates and/or mothers (Dajani & Magann, 2014; Gherman et al., 2006; W. R. Trevathan, 1988)

Here we investigate whether humans have evolved adaptive features in the shoulders to ease obstetrical difficulties, as is the case with the fetal head. The critical obstetrical dimension is fetal shoulder width, which varies to some extent with shoulder position, but is constrained by clavicular length. While clavicular growth from prenatal to postnatal stages has been studied in humans mainly as a measure to estimate the age at death (Black & Scheuer, 1996; Fazekas & Kósa, 1978; Feld et al., 2020; Sherer et al., 2006; Yarkoni et al., 1985), the obstetrical relevance of clavicular growth trajectories remains unknown. Specifically, we hypothesize that, in humans, the prenatal development of the shoulders is obstetrically constrained. To test this hypothesis, we investigate the developmental trajectory of the shoulders from fetal to adult stages in humans, chimpanzees, and Japanese macaques. These species show conspicuous differences in obstetrical constraints related to head and shoulder dimensions (Table 3.1), thus permitting the identification of childbirth-related developmental traits of the shoulders and head. In great apes, the broad shoulders do not complicate childbirth since neonatal size is small relative to maternal pelvic size,

which stands in contrast to the large fetopelvic proportions in humans (DeSilva, 2011; Schultz, 1949). Macaques show a contrasting pattern to humans and great apes. They exhibit comparatively narrow shoulders, with the scapula located laterally on the trunk (Kagaya et al., 2010). Neonates are large relative to mothers, and the neonatal head dimensions are comparable to the maternal pelvic inlet dimensions, resulting in obstetric constraints (DeSilva & Lesnik, 2008; Gherman et al., 2006; Ouzounian & Gherman, 2005; Øverland et al., 2012; Rosenberg, 1992; Rosenberg & Trevathan, 2002; Schultz, 1949; W. Trevathan & Rosenberg, 2000; Chapter 2).

Materials and methods

Sample, volumetric data acquisition, and image data segmentation

The sample consists of whole-body specimens of humans (*Homo sapiens*; $N = 81$), chimpanzees (*Pan troglodytes*; $N = 64$), and Japanese macaques (*Macaca fuscata*; $N = 31$) ranging from late fetal to adult stages. See SI, Fig. S3.1 and Table S3.1 for details. The sample was collected from the following institutions; humans (fetal individuals): the Congenital Anomaly Research Center at Kyoto University Graduate School of Medicine, Japan (Yamaguchi & Yamada, 2018); humans (prenatal and postnatal individuals): the digital autopsy database of University Hospitals Leuven, Belgium; chimpanzees (prenatal and postnatal individuals): Department of Anthropology at University of Zurich, Switzerland (DAUZH); Primate Research Institute of Kyoto University, Japan (KUPRI); Japanese macaques: KUPRI. This study was approved by the ethics committee of Faculty and Graduate School of Medicine of Kyoto University for the use of human fetal specimens (#R0347). All the data from human individuals were anonymized prior to the present study.

The specimens were scanned using medical Computed Tomography (CT) scanners (specimens of KUPRI: Canon Medical Systems; other specimens: Siemens or Philips). The CT scanning and image-reconstruction parameters are as follows: beam collimation 0.5–5.0 mm, slice reconstruction interval 0.2–1.5 mm, reconstruction kernels ("bone" kernels; Canon: FC30/FC31, Siemens/ Philips: B60s). Small specimens of DAUZH (length < 150 mm and diameter < 740 mm) were scanned using a micro-CT scanner (μCT80, Scanco Medical, Switzerland), and volume data were reconstructed at an isotropic voxel resolution of 75 μm.

3D-surfaces of the ossified structures were segmented from the CT volumetric data by setting a bone threshold, then applying the marching-cubes algorithm with the half-maximum threshold criterion, as implemented in Amira 2019.1 (Thermo Fischer Scientific).

Assessment of developmental stage

To compare the developmental patterns between prenatal and postnatal periods, we divided the entire sample into prenatal and postnatal subsamples. Since the age at death was unknown except for the anonymized human subsample, we used skeletal features to differentiate prenatal and postnatal individuals. For humans, we used the status of the tympanic ring as an indicator of developmental stage; fusion of the tympanic ring and squamous plate begins around the gestational age of 35 weeks and it is completed in most of the neonates (Anson et al., 1955). We categorized individuals with incomplete fusion of tympanic ring and squamous plate as fetuses and those with complete tympanic rings as postnatal specimens. For chimpanzees and Japanese macaques, we used the status of the metopic suture as an indicator. The metopic suture closes often shortly after birth and it is partially or completely fused before the eruption of the first deciduous tooth in most of the chimpanzees (Falk et al., 2012) and Japanese macaques, and the first deciduous tooth erupts at the postnatal age of 1.5 months in chimpanzees, and 20 days in Japanese macaques on average (Ashley-Montagu, 1937; Holly Smith et al., 1994; Krogman, 1930) . We categorized chimpanzee and Japanese macaque specimens with a fused metopic suture as postnatal individuals.

Morphometric data acquisition and analysis

To track skeletal growth, we took the following measurements on the virtual three-dimensional models of the whole-body skeleton: cranial length, clavicular length, shoulder width, humeral and femoral length, pelvic width, and trunk length (See Fig. 3.1). The shoulder width was measured as the linear distance between the most lateral points on the proximal epiphyseal lines of the left and right humeri (Fig. 3.1). Because the shoulder girdle is a mobile anatomical unit, direct measurements of its maximum width tend to depend on its postmortem position relative to the trunk. We therefore use the clavicular length as a dimension that constrains the shoulder width independent of shoulder position. SI, Fig. S3.2 shows a tight correlation between the shoulder width and clavicular length, such that the latter measurement serves as a proxy for the former. The clavicular length was measured as the linear distance between the center of the sternal and acromial articular facets (Fig. 3.1). The humeral and femoral lengths were measured as linear distances between the proximal and distal ends on epiphyseal lines (Fig. 3.1). The pelvic width was measured as the linear (Euclidean) distance between the most lateral point of the right and left iliac blades (Fig. 3.1). The trunk length was measured as the sum of linear distances between the most antero-superior points of the following segments: C1 (the first cervical vertebra) to T1 (the first thoracic vertebra), T1 to T5, T5 to L1 (the first lumber vertebra), and L1 to the most antero-inferior point of the last lumbar vertebra (Fig. 3.1). All landmarks used in this study were

set on the CT-based 3D surfaces representing the ossified skeletal structures (Fig. 3.1 and SI, Table S3.2). All linear distances were calculated as Euclidean distances between anatomical landmarks, using a MATLAB-based in-house program, ForMATit (MathWorks, Version R2019b). See Fig. 3.1 and SI, Table S3.2 for definitions of landmarks.

Using the trunk length as a proxy of obstetrically unconstrained body dimensions, we evaluated taxon-specific ontogenetic allometric trajectories of the clavicular length, pelvic width, humeral length, and femoral length (Figs. 3.2, 3.3). Least-square regressions were calculated for prenatal and postnatal periods on logarithmized dimensions (natural logarithm). We performed *F* tests to evaluate whether the slope *a* of the regression line differs significantly from 1 ($p < 5\%$). Slopes $a > 1$ and $a < 1$ indicate positive and negative ontogenetic allometric growth, respectively, whereas slopes that are not statistically different from 1 indicate isometric growth. We revealed further detail of changes in relative skeletal growth rates along ontogenetic trajectories by plotting the log-ratios of clavicular length, pelvic width, and cranial length to trunk length (Fig. 3.3). The resulting slopes $a' = a-1$, which were drawn using the moving average, are positive/negative for positive/negative ontogenetic allometry, respectively, and zero for isometry. All the calculations were performed using MATLAB.

We measured cranial and postcranial skeletal dimensions in ontogenetic series of humans, chimpanzees, and Japanese macaques comprising fetal to adult stages. All measurements were taken on three-dimensional skeletal models derived from Computed Tomography (CT) data of cadaveric specimens (see Fig. 3.1, SI, Fig. S3.1, Table S3.1, and Materials and Methods). The shoulder girdle is a mobile structure, such that direct width measurements are influenced to some extent by its position and orientation relative to the trunk. We therefore use the clavicular length as an additional static measure for shoulder width. The growth characteristics of the shoulders are compared with those of the head (obstetrically constrained), and those of the pelvis, humerus, and femur (obstetrically unconstrained). Trunk length (Fig. 3.1) serves as a reference for obstetrically unconstrained overall body growth. If the growth of the human shoulders is obstetrically constrained, we expect that its growth characteristics deviate from those of the obstetrically unconstrained postcranial skeletal elements.

Results

Growth trajectories were evaluated in two ways. First, we compared prenatal and postnatal ontogenetic allometric trajectories to characterize taxon-specific ontogenies and potential birth-related modifications (Fig. 3.2). Second, we focused on changes in growth rates around birth to further investigate potential obstetric constraints during the transition from prenatal to postnatal

growth characteristics (Figs. 3.3, 3.4). Figures 3.2, 3.3, and Table 3.2 show taxon-specific growth trajectories of the shoulders, cranium, pelvis, and long bones. In humans, the clavicular length exhibits negative ontogenetic allometry relative to the trunk before birth, and positive allometry after birth [Fig. 3.2A, Table 3.2; no statistical difference between males and females (*F* test and ANCOVA; SI, Fig. S3.3 and Table S3.3)]. In chimpanzees, the clavicular length increases isometrically with trunk length, whereas in Japanese macaques the growth characteristics of the shoulders change from prenatal isometry to postnatal negative allometry (Fig. 3.2A, Table 3.2).

In humans, fetal cranial length and shoulder width grow in concordance (i.e., isometrically) and reach similar values around birth (Fig. 3.4), confirming the notion that head and shoulders are exposed to similar obstetric constraints (W. Trevathan & Rosenberg, 2000). After birth, cranial length grows at a lower rate than shoulder width, resulting in a negative allometric relationship that reflects reduced brain growth rate (Fig. 3.4). In chimpanzees and Japanese macaques, cranial length grows at lower rates than shoulder dimensions already before birth (Fig. 3.4).

In all the taxa studied here, the pelvis grows isometrically relative to the trunk during the prenatal period, and it shows positive allometry during the postnatal period (Figs. 3.2B, 3.3B, and Table 3.2). The humerus grows isometrically relative to the trunk during the prenatal period in all the taxa studied here (Fig. 3.2C, Table 3.2). During the postnatal period, it grows with positive allometry in humans and chimpanzees, while it continues along an isometric trajectory in Japanese macaques (Fig. 3.2C, Table 3.2). The human femur grows with moderate positive allometry relative to the trunk during the prenatal period, and with marked positive allometry during the postnatal period, reflecting high lower limb extension rates resulting in the characteristic adult human body proportions (Fig. 3.2D, Table 3.2). In chimpanzees, the femur shows isometric, and moderate positive allometric growth during prenatal and postnatal periods, respectively (Fig. 3.2D, Table 3.2). In Japanese macaques, the femur shows an isometric growth during both prenatal and postnatal periods (Fig. 3.2D, Table 3.2).

Fig. 3.3 shows growth trajectories of relative clavicular, pelvic, and skull dimensions as functions of trunk length. The human-specific pattern of prenatal negative and postnatal positive allometry of the shoulders becomes manifest as a marked decrease of growth rates before birth followed by an increase after birth (Fig. 3.3A). In humans, such a perinatal growth depression is found only in the clavicular length (Fig. 3.3A), while relative pelvic width and relative cranial length increase and decrease, respectively (Figs. 3.3B, C). The clavicular perinatal growth depression is not found in chimpanzees and Japanese macaques (Fig. 3.3A). In chimpanzees, the clavicular length is fairly constant relative to trunk length, while it declines after birth in Japanese

macaques. In chimpanzees and Japanese macaques, growth trajectories of relative pelvic width and relative cranial length are largely similar, respectively, to those found in humans: pelvic width shows a pattern of constant increase relative to trunk length throughout ontogeny (Fig. 3.3B), while the cranial length shows a marked decline relative to trunk length after birth (Fig. 3.3C).

Discussion

Our results revealed a human-specific mode of shoulder growth, that is, a combination of prenatal negative and postnatal positive allometry (Fig. 3.2A, SI, Fig. S3.4) relative to trunk length, and a growth depression around birth (Fig. 3.3A). These growth characteristics are exclusive to the shoulders, and not present in structures not involved in obstetrical complications such as the neonatal pelvis and long bones. Shoulder girdle and pelvic dimensions have been shown to covary in adult non-human primates, indicating correlated growth patterns (Agosto & Auerbach, 2021). On the other hand, the relatively independent modes of human shoulder and pelvic ontogenies around birth (Figs. 3.3A, 3.3B) likely indicate a higher degree of developmental modularity of the shoulder and pelvis in humans compared to non-human primates [(M. Grabowski & Roseman, 2015); M. W. Grabowski et al. (2011); also see Young et al. (2010) showing reduced integration of limb development in humans and apes compared to monkeys]. However, perinatal developmental modularity (as observed here) and adult morphological integration [as observed in Agosto and Auerbach (2021)] do not contradict each other but rather represent different aspects of developmental coordination along the same ontogenetic trajectory. The perinatal growth depression of the human shoulder consists of a prenatal phase of growth deceleration followed by a postnatal phase of growth acceleration (Fig. 3.3A). This latter "catch-up" phase effectively re-establishes the correlation between pelvic, shoulder and limb bone dimensions that is observed in adults (Agosto & Auerbach, 2021; Mallard et al., 2017).

In any case, the human shoulder ontogeny cannot be explained by a generalized primate mode of postcranial ontogeny and likely represents a developmental feature that keeps the neonatal shoulders at the same width as the obstetrically relevant dimensions of the neonatal head (Fig. 3.4). In contrast to humans, neither chimpanzees nor Japanese macaques show a perinatal growth depression of the shoulders (Fig. 3.3A). The observed taxon-specific patterns of ontogenetic allometry (Figs. 3.3, 3.4, Table 3.2) are consistent with differences in obstetrical conditions and in adult shoulder width (Table 3.1): The broad shoulders of adult chimpanzees are achieved by maintaining the same growth rate (i.e., isometric growth relative to trunk length) throughout prenatal and postnatal ontogeny while those of humans are achieved by decelerated prenatal and accelerated postnatal development. Collectively, these results support the hypothesis

that in humans the widening of the shoulder girdle during the prenatal period is constrained to ease obstetrical difficulties, while the postnatal growth "catch-up" yields wide adult shoulders (Figs. 3,2A, 3.3A).

If the perinatal growth depression of the human shoulders reflects an obstetrical adaptation, then why does the problem of shoulder dystocia persist? We hypothesize that human shoulder width faces a similar obstetrical dilemma as the head, i.e., an evolutionary conflict between selective pressures favoring large neonatal head (and shoulder) dimensions and pressures limiting birth canal dimensions, as proposed by the cliff-edge model for the evolution of fetopelvic proportions (Mitteroecker et al., 2016). Directional selection for wide neonatal shoulders could have several reasons. For humans, it has been argued that wide shoulders function to stabilize the trunk during bipedal locomotion and to facilitate high-speed throwing (Bramble & Lieberman, 2004; Roach et al., 2013). Another possible explanation could come from respiratory requirements. It is likely that shoulder width is functionally and developmentally linked to the size of the thorax. To initiate and sustain postnatal respiratory function, a certain size of the thorax is required. Thoracic growth disorder is one of the causes of the thoracic insufficiency syndrome, defined as the inability of the thorax to support normal respiration or lung growth (Campbell Jr et al., 2003).

When then did the mode of shoulder development observed in modern humans emerge in the hominin lineage? DeSilva et al. (2017) proposed that *Australopithecus afarensis* could have had an elevated risk of the shoulder dystocia, based on estimates of the neonatal shoulder width. Following this proposition, we hypothesize that the prenatal restriction of shoulder growth evolved in the australopithecines. There is evidence that *A. africanus* exhibited a delayed fusion of the metopic suture (Falk et al., 2012) [but see Holloway et al. (2014)], which would indicate that obstetric adaptations of the head and shoulders evolved in concert. These scenarios, however, remain to be tested with ontogenetic data of an expanded sample of primate species representing a wide range of shoulder width (Kagaya et al., 2010). For example, gibbons also have wide shoulders, and there is a tight fit between neonate head to maternal pelvic dimensions (Schultz, 1949). Further studies will test the hypothesis that gibbons exhibit a similar perinatal mode of shoulder development as reported here for humans.

While the key obstetric adaptation of the human shoulders consists in a perinatal growth rate depression, the obstetric ontogenetic adaptation of the human head exhibits a different pattern. Prenatal brain growth in chimpanzees and macaques follows the typical trajectory of precocial mammals, where cerebral peak growth rates are reached long before birth (while in altricial mammals, they are reached after birth) (Halley, 2017; Sakai et al., 2012). Interestingly, brain

growth in humans also follows the precocial pattern with a prenatal cerebral growth peak (Halley, 2017), but compared to non-human primates, the peak is close to birth (Halley, 2017; Sakai et al., 2012). As an effect, human fetuses grow comparatively large heads, while growth rate reduction shortly before birth results in obstetrically compatible head dimensions. This pattern can be explained by each of the two main hypotheses on fetal cranial development: obstetrical constraints (Washburn, 1960) and maternal metabolic constraints (Holly M. Dunsworth et al., 2012). Accordingly, the late prenatal timing of the human cerebral peak growth rate likely reflects a compromise between extended fetal brain growth on the one hand, and maternal pelvic and metabolic constraints on the other.

In sum, we propose that human shoulder and head ontogenies both show evidence of obstetric adaptations, but with different evolutionary foundations. The perinatal depression of shoulder growth rate is found only in humans (Figs. 3.2A, 3.3A) and likely evolved in the hominin lineage. In contrast, the prenatal decline of brain growth rate represents a primitive mode of ontogeny shared with other primates, which was pushed toward the limits imposed by obstetrical and/or maternal metabolic constraints. Together, these mechanisms result in a close match of the obstetrically relevant dimensions of the neonatal shoulders and skull (Fig. 3.4).

This study has explored the intricate effects of obstetric constraints on human fetal development and neonate body shape. Further studies are required to elucidate whether fetal–maternal obstetric and metabolic constraints had even more pervasive effects on human ontogeny and developmental modularity and integration (Mallard et al., 2017), and to which extent they represent evolutionary adaptations versus developmental plasticity.

References

Abitbol, M. M. (1988). Evolution of the ischial spine and of the pelvic floor in the hominoidea. *American Journal of Physical Anthropology, 75*(1), 53-67. doi:10.1002/ajpa.1330750107

Agosto, E. R., & Auerbach, B. M. (2021). Evolvability and constraint in the primate basicranium, shoulder, and hip and the importance of multi-trait evolution. *Evolutionary Biology, 48*(2), 221-232.

Alentorn-Geli, E., Myer, G. D., Silvers, H. J., Samitier, G., Romero, D., Lázaro-Haro, C., & Cugat, R. (2009). Prevention of non-contact anterior cruciate ligament injuries in soccer players. Part 1: Mechanisms of injury and underlying risk factors. *Knee Surgery, Sports Traumatology, Arthroscopy, 17*(7), 705-729. doi:10.1007/s00167-009-0813-1

Ami, O., Maran, J. C., Gabor, P., Whitacre, E. B., Musset, D., Dubray, C., Mage, G., & Boyer, L. (2019). Three-dimensional magnetic resonance imaging of fetal head molding and brain shape changes during the second stage of labor. *PLOS ONE, 14*(5).

Anson, B. J., Bast, T. H., & Richany, S. F. (1955). The fetal and early postnatal development of the tympanic ring and related structures in man. *Annals of Otology, Rhinology & Laryngology, 64*(3), 802-823.

Ashley-Montagu, M. F. (1937). The medio-frontal suture and the problem of metopism in the primates. *The Journal of the Royal Anthropological Institute of Great Britain and Ireland, 67*, 157-201. doi:10.2307/2844176

Beischer, N. A. (1986). *Obstetrics and the newborn: an illustrated textbook*: Saunders.

Bérard, J., Dufour, P., Vinatier, D., Subtil, D., Vanderstichèle, S., Monnier, J. C., & Puech, F. (1998). Fetal macrosomia: risk factors and outcome: A study of the outcome concerning 100 cases>4500 g. *European Journal of Obstetrics & Gynecology and Reproductive Biology, 77*(1), 51-59. doi:https://doi.org/10.1016/S0301-2115(97)00242-X

BjöRklund, K., Lindgren, P. G., BergströM, S., & Ulmsten, U. (1997). Sonographic assessment of symphyseal joint distention intra partum. *Acta Obstetricia et Gynecologica Scandinavica, 76*(4), 227-232. doi:10.3109/00016349709047800

Black, S., & Scheuer, L. (1996). Age changes in the clavicle: from the early neonatal period to skeletal maturity. *International Journal of Osteoarchaeology, 6*(5), 425-434. doi:https://doi.org/10.1002/(SICI)1099-1212(199612)6:5<425::AID-OA287>3.0.CO;2-U

Bramble, D. M., & Lieberman, D. E. (2004). Endurance running and the evolution of *Homo*. *Nature, 432*(7015), 345-352. doi:10.1038/nature03052

Brown, K. M., Handa, V. L., Macura, K. J., & DeLeon, V. B. (2013). Three-dimensional shape differences in the bony pelvis of women with pelvic floor disorders. *International urogynecology journal, 24*(3), 431-439.

Campbell Jr, R. M., Smith, M. D., Mayes, T. C., Mangos, J. A., Willey-Courand, D. B., Kose, N., Pinero, R. F., Alder, M. E., Duong, H. L., & Surber, J. L. (2003). The characteristics of thoracic insufficiency syndrome associated with fused ribs and congenital scoliosis. *JBJS, 85*(3), 399-408.

Chopra, S. R. K. (1957). The cranial suture closure in monkeys. *Proceedings of the Zoological Society of London, 128*(1), 67-112. doi:10.1111/j.1096-3642.1957.tb00257.x

Correia, H., Balseiro, S., & De Areia, M. (2005). Sexual dimorphism in the human pelvis: Testing a new hypothesis. *HOMO, 56*(2), 153-160. doi:https://doi.org/10.1016/j.jchb.2005.05.003

Dajani, N. K., & Magann, E. F. (2014). Complications of shoulder dystocia. *Seminars in Perinatology, 38*(4), 201-204. doi:https://doi.org/10.1053/j.semperi.2014.04.005

DeSilva, J. M. (2011). A shift toward birthing relatively large infants early in human evolution. *Proceedings of the National Academy of Sciences, 108*(3), 1022-1027. doi:10.1073/pnas.1003865108

DeSilva, J. M., Laudicina, N. M., Rosenberg, K. R., & Trevathan, W. R. (2017). Neonatal shoulder width suggests a semirotational, oblique birth mechanism in *Australopithecus afarensis*. *The Anatomical Record, 300*(5), 890-899. doi:10.1002/ar.23573

DeSilva, J. M., & Lesnik, J. J. (2008). Brain size at birth throughout human evolution: A new method for estimating neonatal brain size in hominins. *Journal of Human Evolution, 55*(6), 1064-1074. doi:https://doi.org/10.1016/j.jhevol.2008.07.008

Dunsworth, H. M. (2018). There is no" obstetrical dilemma": Towards a braver medicine with fewer childbirth interventions. *Perspectives in biology and medicine, 61*(2), 249-263.

Dunsworth, H. M., Warrener, A. G., Deacon, T., Ellison, P. T., & Pontzer, H. (2012). Metabolic hypothesis for human altriciality. *Proceedings of the National Academy of Sciences, 109*(38), 15212-15216. doi:10.1073/pnas.1205282109

Ezegwui, H., Ikeako, L., & Egbuji, C. (2011). Fetal macrosomia: obstetric outcome of 311 cases in UNTH, Enugu, Nigeria. *Nigerian journal of clinical practice, 14*(3), 322-326.

Falk, D., Zollikofer, C. P. E., Morimoto, N., & Ponce de León, M. S. (2012). Metopic suture of Taung (*Australopithecus africanus*) and its implications for hominin brain evolution. *Proceedings of the National Academy of Sciences, 109*(22), 8467-8470. doi:10.1073/pnas.1119752109

Fazekas, I. G., & Kósa, F. (1978). *Forensic fetal osteology*: Akadémiai Kiadó.

Feld, K., Bonni, M., Körber, F., Eifinger, F., & Banaschak, S. (2020). Post-mortem estimation of

gestational age and maturation of new-borns by CT examination of clavicle length, femoral length and femoral bone nuclei. *Forensic Science International, 314*, 110391. doi:https://doi.org/10.1016/j.forsciint.2020.110391

Fischer, B., & Mitteroecker, P. (2015). Covariation between human pelvis shape, stature, and head size alleviates the obstetric dilemma. *Proceedings of the National Academy of Sciences, 112*(18), 5655-5660. doi:10.1073/pnas.1420325112

Gherman, R. B., Chauhan, S., Ouzounian, J. G., Lerner, H., Gonik, B., & Goodwin, T. M. (2006). Shoulder dystocia: The unpreventable obstetric emergency with empiric management guidelines. *American Journal of Obstetrics and Gynecology, 195*(3), 657-672. doi:https://doi.org/10.1016/j.ajog.2005.09.007

Grabowski, M., & Roseman, C. C. (2015). Complex and changing patterns of natural selection explain the evolution of the human hip. *Journal of Human Evolution, 85*, 94-110. doi:https://doi.org/10.1016/j.jhevol.2015.05.008

Grabowski, M. W., Polk, J. D., & Roseman, C. C. (2011). Divergent patterns of integration and reduced constraint in the human hip and the origins of bipedalism. *Evolution, 65*(5), 1336-1356.

Gross, T. L., Sokol, R. J., Williams, T., & Thompson, K. (1987). Shoulder dystocia: A fetal-physician risk. *American Journal of Obstetrics and Gynecology, 156*(6), 1408-1418. doi:https://doi.org/10.1016/0002-9378(87)90008-1

Halley, A. C. (2017). Minimal variation in eutherian brain growth rates during fetal neurogenesis. *Proceedings of the Royal Society B: Biological Sciences, 284*(1854), 20170219.

Holloway, R. L., Broadfield, D. C., & Carlson, K. J. (2014). New high-resolution computed tomography data of the Taung partial cranium and endocast and their bearing on metopism and hominin brain evolution. *Proceedings of the National Academy of Sciences, 111*(36), 13022-13027. doi:10.1073/pnas.1402905111

Holly Smith, B., Crummett, T. L., & Brandt, K. L. (1994). Ages of eruption of primate teeth: a compendium for aging individuals and comparing life histories. *American Journal of Physical Anthropology, 37*(S19), 177-231.

Huseynov, A., Zollikofer, C. P. E., Coudyzer, W., Gascho, D., Kellenberger, C., Hinzpeter, R., & Ponce de León, M. S. (2016). Developmental evidence for obstetric adaptation of the

human female pelvis. *Proceedings of the National Academy of Sciences, 113*(19), 5227-5232. doi:10.1073/pnas.1517085113

Ju, H., Chadha, Y., Donovan, T., & O'rourke, P. (2009). Fetal macrosomia and pregnancy outcomes. *Australian and New Zealand Journal of Obstetrics and Gynaecology, 49*(5), 504-509. doi:https://doi.org/10.1111/j.1479-828X.2009.01052.x

Kagaya, M., Ogihara, N., & Nakatsukasa, M. (2010). Is the clavicle of apes long? An investigation of clavicular length in relation to body mass and upper thoracic width. *International Journal of Primatology, 31*(2), 209-217.

Krogman, W. M. (1930). Studies in growth changes in the skull and face of anthropoids. II. Ectocranial and endocranial suture closure in anthropoids and Old World Apes. *American Journal of Anatomy, 46*(2), 315-353. doi:10.1002/aja.1000460206

Laudicina, N. M., & Cartmill, M. (2019). *Obstetric constraints in large-brained cebids and modern humans: A comparison of coping mechanisms.* Paper presented at the American Journal of Physical Anthropology.

LaVelle, M. (1995). Natural selection and developmental sexual variation in the human pelvis. *American Journal of Physical Anthropology, 98*(1), 59-72. doi:https://doi.org/10.1002/ajpa.1330980106

Mallard, A. M., Savell, K. R. R., & Auerbach, B. M. (2017). Morphological integration of the human pelvis with respect to age and sex. *The Anatomical Record, 300*(4), 666-674. doi:https://doi.org/10.1002/ar.23547

Mitteroecker, P., Huttegger, S. M., Fischer, B., & Pavlicev, M. (2016). Cliff-edge model of obstetric selection in humans. *Proceedings of the National Academy of Sciences, 113*(51), 14680-14685. doi:doi:10.1073/pnas.1612410113

Moffett, E. A. (2017). Dimorphism in the size and shape of the birth canal across anthropoid primates. *The Anatomical Record, 300*(5), 870-889. doi:10.1002/ar.23572

Ouzounian, J. G., & Gherman, R. B. (2005). Shoulder dystocia: Are historic risk factors reliable predictors? *American Journal of Obstetrics and Gynecology, 192*(6), 1933-1935. doi:https://doi.org/10.1016/j.ajog.2005.02.054

Øverland, E. A., Vatten, L. J., & Eskild, A. (2012). Risk of shoulder dystocia: associations with parity and offspring birthweight. A population study of 1 914 544 deliveries. *Acta*

Obstetricia et Gynecologica Scandinavica, 91(4), 483-488. doi:https://doi.org/10.1111/j.1600-0412.2011.01354.x

Pavličev, M., Romero, R., & Mitteroecker, P. (2020). Evolution of the human pelvis and obstructed labor: new explanations of an old obstetrical dilemma. *American Journal of Obstetrics & Gynecology, 222*(1), 3-16. doi:10.1016/j.ajog.2019.06.043

Roach, N. T., Venkadesan, M., Rainbow, M. J., & Lieberman, D. E. (2013). Elastic energy storage in the shoulder and the evolution of high-speed throwing in Homo. *Nature, 498*(7455), 483-486.

Rosenberg, K. (1992). The evolution of modern human childbirth. *American Journal of Physical Anthropology, 35*(S15), 89-124. doi:10.1002/ajpa.1330350605

Rosenberg, K., & Trevathan, W. (2002). Birth, obstetrics and human evolution. *BJOG: An International Journal of Obstetrics & Gynaecology, 109*(11), 1199-1206. doi:10.1046/j.1471-0528.2002.00010.x

Ruff, C. B. (1995). Biomechanics of the hip and birth in early *Homo*. *American Journal of Physical Anthropology, 98*(4), 527-574. doi:10.1002/ajpa.1330980412

Sakai, T., Hirata, S., Fuwa, K., Sugama, K., Kusunoki, K., Makishima, H., Eguchi, T., Yamada, S., Ogihara, N., & Takeshita, H. (2012). Fetal brain development in chimpanzees versus humans. *Current Biology, 22*(18), R791-R792. doi:https://doi.org/10.1016/j.cub.2012.06.062

Sandmire, H. F., & O'Halloin, T. J. (1988). Shoulder dystocia: its incidence and associated risk factors. *International Journal of Gynecology & Obstetrics, 26*(1), 65-73. doi:https://doi.org/10.1016/0020-7292(88)90198-1

Schultz, A. H. (1949). Sex differences in the pelves of primates. *American Journal of Physical Anthropology, 7*(3), 401-424. doi:10.1002/ajpa.1330070307

Sherer, D. M., Sokolovski, M., Dalloul, M., Khoury-Collado, F., Osho, J. A., Lamarque, M. D., & Abulafia, O. (2006). Fetal clavicle length throughout gestation: a nomogram. *Ultrasound in Obstetrics & Gynecology, 27*(3), 306-310. doi:https://doi.org/10.1002/uog.2706

Sjöberg, I., Erichs, K., & BJerre, I. (1988). Cause and effect of obstetric (neonatal) brachial plexus palsy. *Acta Paediatrica, 77*(3), 357-364. doi:https://doi.org/10.1111/j.1651-

2227.1988.tb10660.x

Stansfield, E., Kumar, K., Mitteroecker, P., & Grunstra, N. D. S. (2021). Biomechanical trade-offs in the pelvic floor constrain the evolution of the human birth canal. *Proceedings of the National Academy of Sciences, 118*(16), e2022159118. doi:doi:10.1073/pnas.2022159118

Stoller, M. K. (1996). The obstetric pelvis and mechanism of labor in nonhuman primates.

Sze, E. H. M., Kohli, N., Miklos, J. R., Roat, T., & Karram, M. M. (1999). Computed tomography comparison of bony pelvis dimensions between women with and without genital prolapse. *Obstetrics & Gynecology, 93*(2), 229-232. doi:https://doi.org/10.1016/S0029-7844(98)00376-7

Tague, R. G., & Lovejoy, C. O. (1986). The obstetric pelvis of A.L. 288-1 (Lucy). *Journal of Human Evolution, 15*(4), 237-255. doi:https://doi.org/10.1016/S0047-2484(86)80052-5

Trevathan, W., & Rosenberg, K. (2000). The shoulders follow the head: postcranial constraints on human childbirth. *Journal of Human Evolution, 39*(6), 583-586. doi:https://doi.org/10.1006/jhev.2000.0434

Trevathan, W. R. (1988). Fetal emergence patterns in evolutionary perspective. *American Anthropologist, 90*(3), 674-681. doi:10.1525/aa.1988.90.3.02a00100

Vidarsdottir, H., Geirsson, R. T., Hardardottir, H., Valdimarsdottir, U., & Dagbjartsson, A. (2011). Obstetric and neonatal risks among extremely macrosomic babies and their mothers. *American Journal of Obstetrics and Gynecology, 204*(5), 423.e421-423.e426. doi:https://doi.org/10.1016/j.ajog.2010.12.036

Washburn, S. L. (1960). Tools and human evolution. *Scientific American, 203*(3), 62-75.

Wittman, A. B., & Wall, L. L. (2007). The evolutionary origins of obstructed labor: Bipedalism, encephalization, and the human obstetric dilemma. *Obstetrical & Gynecological Survey, 62*(11), 739-748. doi:10.1097/01.ogx.0000286584.04310.5c

Yamaguchi, Y., & Yamada, S. (2018). The Kyoto collection of human embryos and fetuses: history and recent advancements in modern methods. *Cells Tissues Organs, 205*(5-6), 314-319.

Yarkoni, S., Schmidt, W., Jeanty, P., Reece, E. A., & Hobbins, J. C. (1985). Clavicular

measurement: a new biometric parameter for fetal evaluation. *Journal of Ultrasound in Medicine, 4*(9), 467-470. doi:https://doi.org/10.7863/jum.1985.4.9.467

Young, N. M., Wagner, G. P., & Hallgrímsson, B. (2010). Development and the evolvability of human limbs. *Proceedings of the National Academy of Sciences, 107*(8), 3400-3405. doi:10.1073/pnas.0911856107

Figures

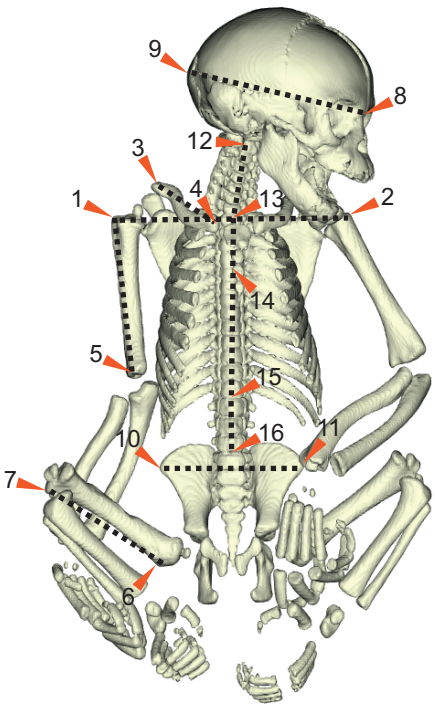

Fig. 3.1 Anatomical landmarks and linear measurements (shown on a neonatal chimpanzee). Red arrow heads indicate landmark locations. Dashed lines indicate linear measurements (shoulder width: #1–#2, clavicular length: #3–#4, humeral length: #1–#5, femoral length: #6–#7, cranial length: #8–#9, pelvic width: #10–#11, and trunk length: sum of segments from #12 to #16). See SI, Table S3.2 for landmark definitions.

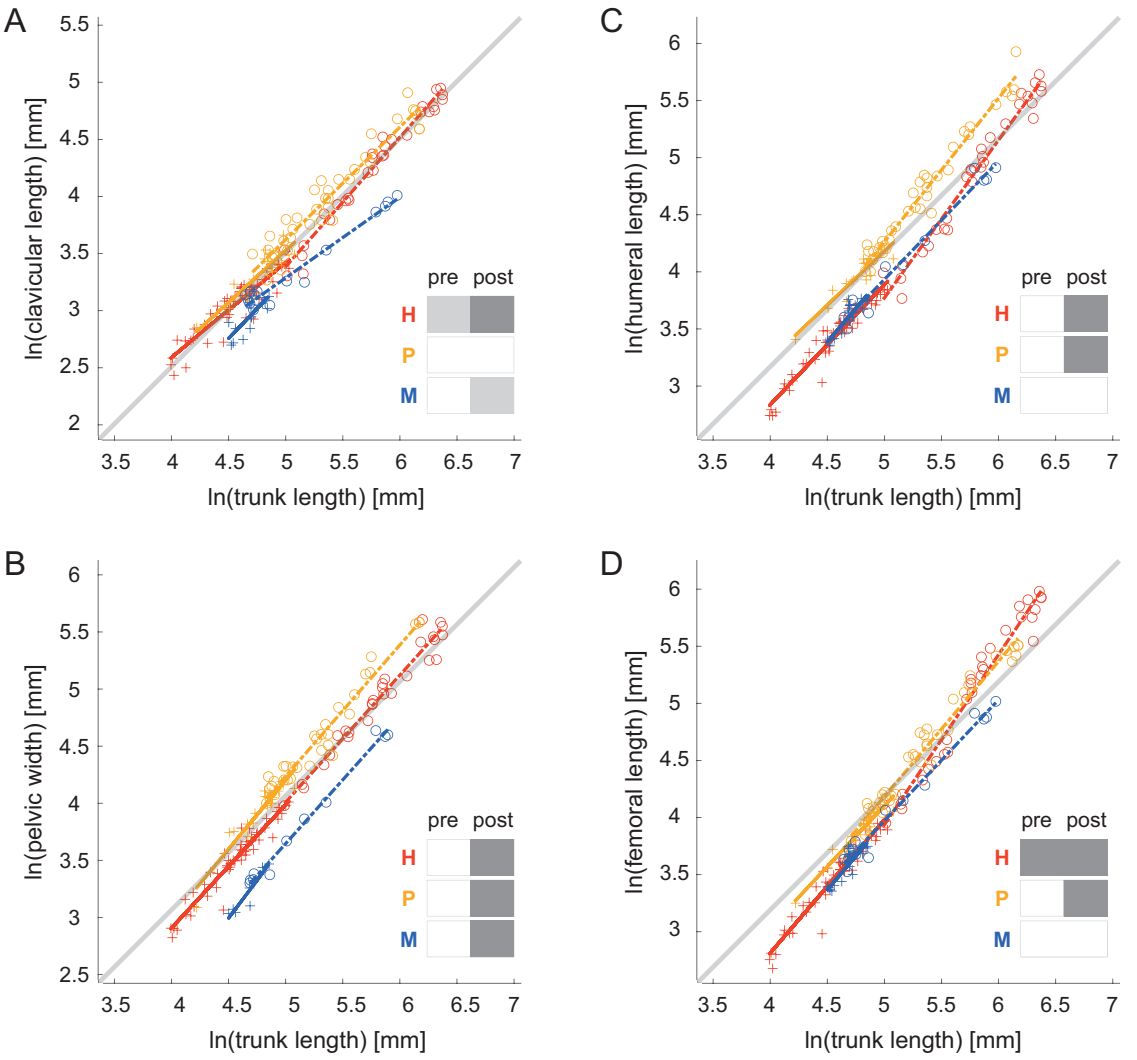

Fig. 3.2 Double-logarithmic plots of clavicular length (*A*), pelvic width (*B*), humeral length (*C*), and femoral length (*D*) versus trunk length. Crosses and circles indicate prenatal (pre) and postnatal (post) specimens, respectively [red: humans (H), yellow: chimpanzees (P), and blue: Japanese macaques (M)]. Least-squares regressions for prenatal and postnatal periods are shown as solid and dashed lines, respectively. Gray solid lines indicate isometric growth (slope = 1). Diagrams in lower-right corner of each plot show ontogenetic allometric characteristics [dark gray/light gray: positive/negative allometry, white: isometry]. Only the human clavicle exhibits prenatal negative and postnatal positive allometric growth characteristics. See also Table 3.2.

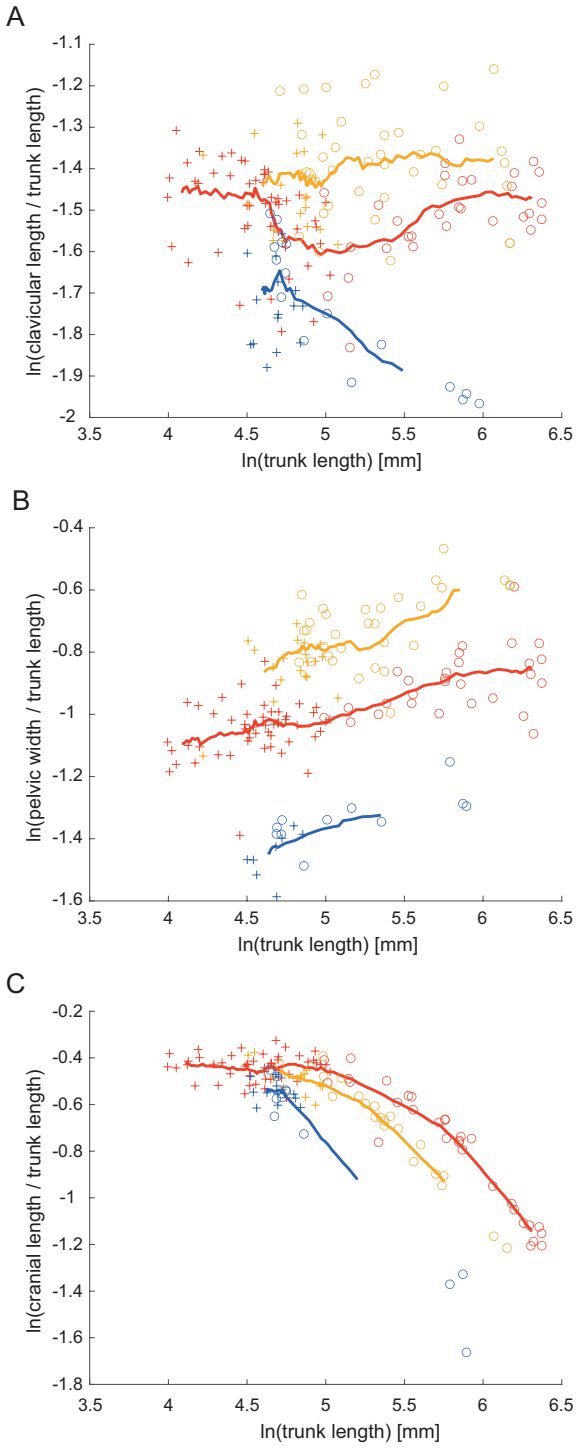

Fig. 3.3 Development of relative clavicular (*A*), pelvic (*B*), and cranial (*C*) dimensions (symbols and colors as in Fig. 3.2; moving-average trajectories). Human clavicular ontogeny is different from that in chimpanzees and Japanese macaques, showing a marked perinatal growth depression. In all species, pelvic width increases linearly relative to trunk length, while cranial length declines rapidly relative to trunk length after birth.

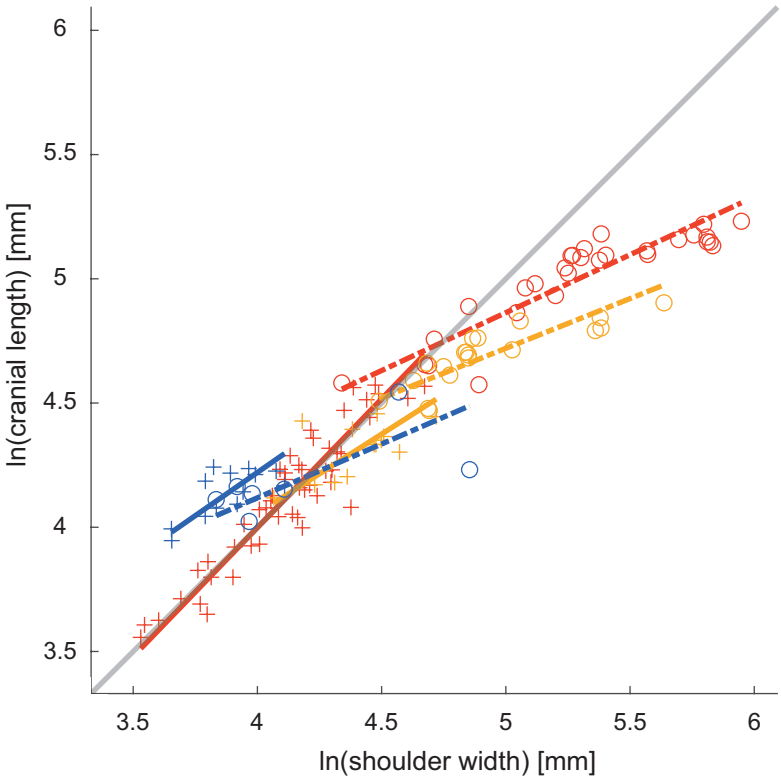

Fig. 3.4 Growth of cranial length relative to shoulder width (symbols and colors as in Fig. 3.2). In humans, shoulder width and cranial length tend to grow along the line of identity (shown in gray) until birth, resulting in similar obstetrically relevant dimensions. Only after birth, human shoulder width exceeds cranial length (see SI, Table S3.4 for details).

Tables

Table 3.1 Obstetrical conditions in humans, chimpanzees, and macaques.

	Neonatal head size relative to birth canal	Shoulder width in adult	Neonatal shoulder width relative to birth canal (inlet)
Humans	large	wide	wide
Chimpanzees	small	wide	narrow
Macaques	large	narrow	narrow

Table 3.2 Taxon-specific ontogenetic allometric patterns [slopes of the regression lines and their standard deviations (in parentheses) of Fig. 3.2]. Colors indicate slopes that are statistically different from 1 ($p < 0.05$); dark gray/light gray: positive/negative allometry.

		prenatal	postnatal
Humans	clavicle	0.83 (0.05)	1.13 (0.04)
	pelvis	1.08 (0.04)	1.11 (0.04)
	humerus	1.05 (0.04)	1.38 (0.05)
	femur	1.17 (0.05)	1.49 (0.05)
Chimpanzees	clavicle	0.91 (0.11)	0.98 (0.05)
	pelvis	1.21 (0.10)	1.15 (0.05)
	humerus	0.95 (0.08)	1.26 (0.04)
	femur	1.07 (0.08)	1.18 (0.04)
Japanese macaques	clavicle	1.05 (0.23)	0.71 (0.04)
	pelvis	1.13 (0.20)	1.12 (0.04)
	humerus	1.18 (0.17)	1.04 (0.05)
	femur	1.18 (0.19)	1.06 (0.05)

Supporting Information

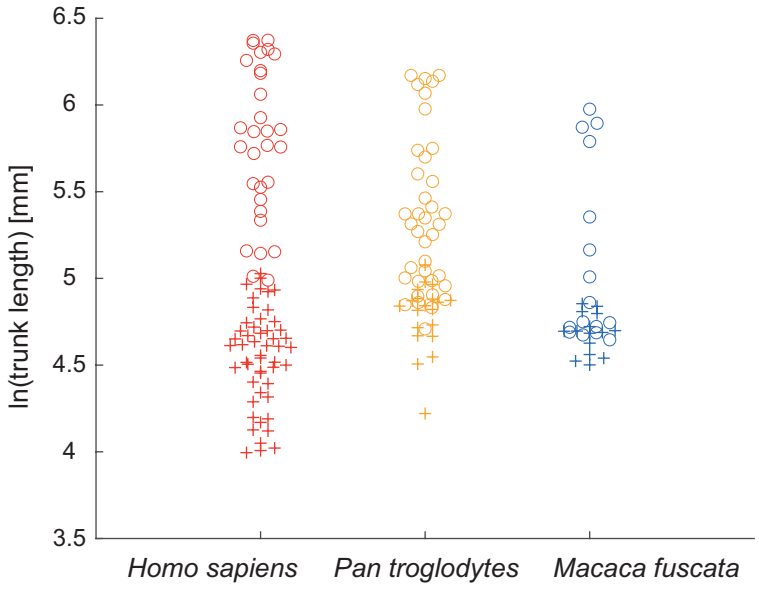

Fig. S3.1 Graphical representation of the sample structure. Distribution of the ontogenetic series is shown by trunk length. Crosses and circles indicate prenatal and postnatal specimens, respectively (red: humans, yellow: chimpanzees, and blue: Japanese macaques).

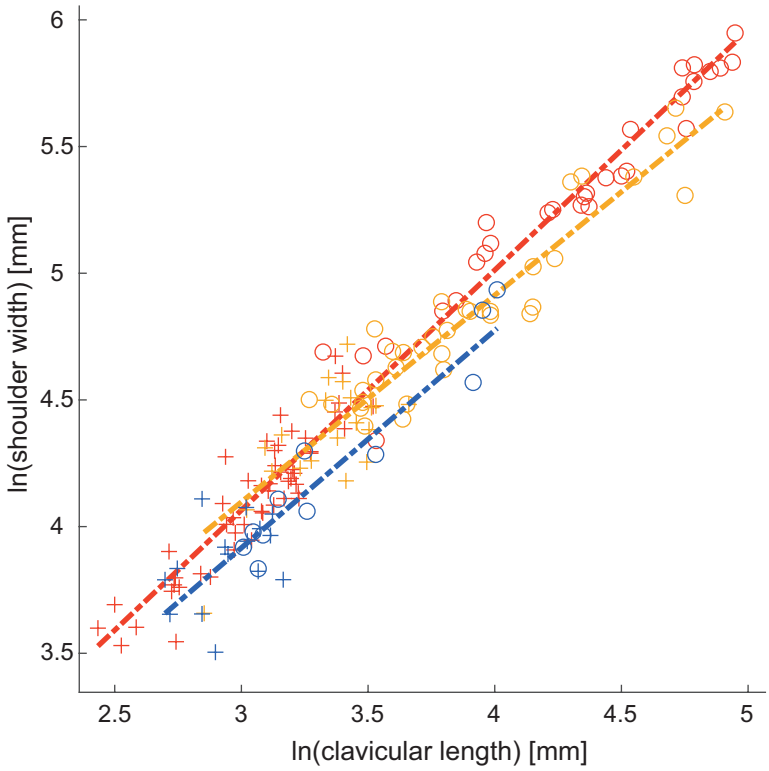

Fig. S3.2 Clavicular length and shoulder width [double-logarithmic plot (natural logarithm)]. The two variables are highly correlated with each other [$R = 0.99$ (humans), $R = 0.95$ (chimpanzees), $R = 0.94$ (Japanese macaques); $P < 0.05$ for all taxa]. Crosses and circles indicate prenatal and postnatal specimens, respectively (red: humans, yellow: chimpanzees, and blue: Japanese macaques). Regression lines were calculated for pooled samples of prenatal and postnatal individuals.

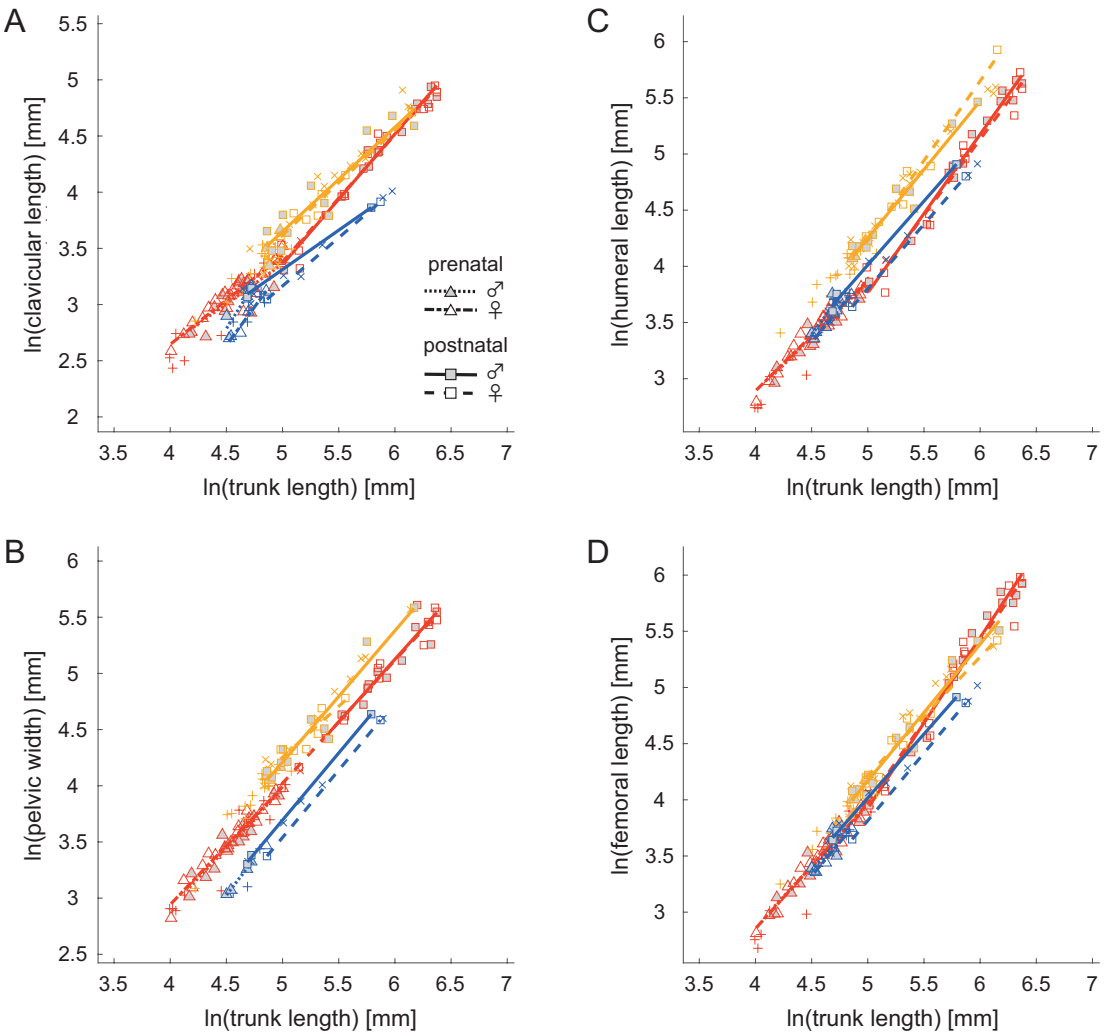

Fig. S3.3 Evaluation of sexual dimorphism [double-logarithmic plot (natural logarithm)]. A: clavicular length, B, pelvic width, C: humeral length, D: femoral length. Colors indicate the different taxa (red: humans, yellow: chimpanzees, and blue: Japanese macaques). Triangles/squares: prenatal/postnatal specimens (gray/open symbols: males/females). +/x marks: prenatal/postnatal specimens with unknown sex. Dotted/solid lines: prenatal/postnatal males. Dash-dotted/dashed lines: prenatal/postnatal females. Lines of ontogenetic allometry are statistically indistinguishable between males and females (*F* test and ANCOVA; see Table S3.3 for *P* values).

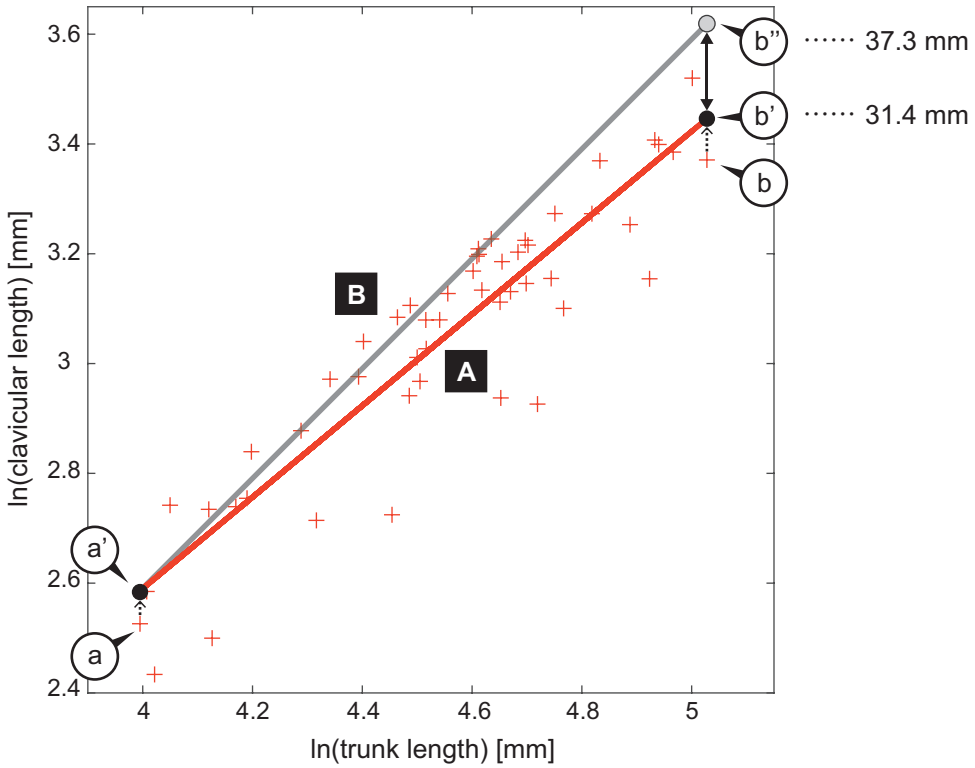

Fig. S3.4 Actual negative allometric and hypothetical isometric prenatal growth trajectories of the human clavicle [double-logarithmic plot (natural logarithm)]. Crosses indicate the prenatal specimens of humans. A (red line): least-squares regression line of the actual ontogenetic trajectory (negative allometry). Points a and b: specimens with smallest and largest trunk length in the human sample, respectively. Points a' and b': predicted clavicular lengths of points a and b on line A. B (gray line): hypothetical isometric growth trajectory (slope = 1) that starts at point a' and ends at point b'' (predicted isometrically grown clavicular length of a). Predicted clavicular lengths at b' and b'' are 31.4 mm and 37.3 mm, respectively. It appears that with the hypothetical isometric growth the clavicular length would be 5.9 mm (i.e., 11.8 mm in total of right and left sides) longer than with actual negative allometric growth (black arrow). The clavicular length at birth predicted by negative allometric growth (point b') is thus approximately 16% shorter than the length predicted by prenatal isometric growth (point b'').

Table S3.1 Sample structure (see also Fig. S3.1).

		N		
Species	Fetus	Postnatal period (immature)	Postnatal period (mature)	Total
Homo sapiens	51	23	7	81
Pan troglodytes	20	34	10	64
Macaca fuscata	15	12	4	31

Table S3.2 Definitions of the landmarks. See also Fig. 3.1.

Landmark numbers	Definitions	Used in measurement of
1	Most lateral and proximal end of epiphyseal line of the right humerus	Shoulder width/Humeral length
2	Most lateral and proximal end of epiphyseal line of the left humerus	Shoulder width
3	Center of the sternal articular facet of the right clavicle	Clavicular length
4	Center of the acromial articular facet of the right clavicle	Clavicular length
5	Most lateral and distal end of epiphyseal line of the right humerus	Humeral length
6	Most lateral and proximal end of epiphyseal line of the right femur	Femoral length
7	Most lateral and distal end of epiphyseal line of the right femur	Femoral length
8	Nasion	Cranial length
9	Opisthocranion	Cranial length
10	Most lateral point of the right iliac blade	Pelvic width
11	Most lateral point of the left iliac blade	Pelvic width
12	Most antero-superior point of the first cervical vertebra	Trunk length
13	Most antero-superior point of the first thoracic vertebra	Trunk length
14	Most antero-superior point of the fifth thoracic vertebra	Trunk length
15	Most antero-superior point of the first lumbar vertebra	Trunk length
16	Most antero-inferior point of the last lumbar vertebra	Trunk length

Table S3.3 Tests of sexual dimorphism in allometric regression lines.

		Prenatal				Postnatal			
		*N**	*F* test	ANCOVA		*N*	*F* test	ANCOVA	
		m/f	Slope	Slope	Intercept	m/f	Slope	Slope	Intercept
Humans	Clavicle	19/20	0.50	0.55	0.20	14/13	0.69	0.74	0.99
	Pelvis	19/20	0.84	0.87	0.33	13/12	0.66	0.85	0.86
	Humerus	19/20	0.96	0.96	0.47	14/13	0.51	0.51	0.45
	Femur	19/20	0.69	0.72	0.91	14/13	0.42	0.53	0.79
Chimpanzees	Clavicle	3/0	-	-	-	11/7	0.95	0.98	0.66
	Pelvis	3/0	-	-	-	10/6	0.32	0.41	0.72
	Humerus	3/0	-	-	-	10/7	0.14	0.22	0.42
	Femur	3/0	-	-	-	11/7	0.18	0.26	0.82
Japanese macaques	Clavicle	4/4	0.76	0.74	0.06	3/2	-	-	-
	Pelvis	4/1	-	-	-	3/2	-	-	-
	Humerus	4/4	0.81	0.78	0.19	3/2	-	-	-
	Femur	4/4	0.96	0.95	0.63	3/2	-	-	-

*Number of specimens with known sex. *F* test and ANCOVA: *P* values of *F* and ANCOVA tests of the difference between male (m) and female (f) ontogenetic allometric regression lines (also see Fig. S3.3). Tests were only conducted for the groups with adequate subsample sizes.

Table S3.4 Slopes of allometric regression of ln(shoulder width) vs. ln(cranial length) (reduced major axis method). Human shoulder and head dimensions exhibit an isometric growth during the prenatal period. The 95% confidence intervals (CI) are shown.

		Slope	CI	
Humans	Prenatal	1.04	0.93	1.15
	Postnatal	0.47	0.39	0.54
Chimpanzees	Prenatal	0.64	0.30	0.98
	Postnatal	0.40	0.29	0.51
Japanese macaques	Prenatal	0.70	0.37	1.02
	Postnatal	0.43	0.06	0.81

Chapter 4
Conclusion

In this thesis, I addressed questions on adaptations to obstetrical constraints in the head and shoulders in primate fetuses and their mothers. The results are summarized as follows:

1. *Does the morphological covariation between the fetal skull and maternal pelvis alleviate obstetrical difficulty?*

   The data of actual mother–fetus dyads of rhesus macaques showed direct evidence of cephalopelvic covariation, supporting the hypothesis proposed for humans by Fischer and Mitteroecker (2015). Birth canal-related locations show a greater degree of cephalopelvic covariation than other locations, which indicates cephalopelvic covariation effectively alleviates obstetrical difficulties.

2. *Is human shoulder development adapted to obstetrical constraints?*

   The cross-sectional ontogenetic data showed that human shoulder development is decelerated before birth but accelerated after birth. This unique developmental pattern likely eases obstetrical difficulties. This indicates that human shoulders, as the head, are faced with obstetrical dilemma: in the shoulder case, trade-off between locomotor and respiratory functions versus safe delivery.

Currently, data from humans and macaques (cephalopelvic covariation and shoulder development) and from chimpanzees (shoulder development) are available to infer the evolutionary scenarios for the patterns of obstetrical adaptation found in these primate species (Fig. 4.1).

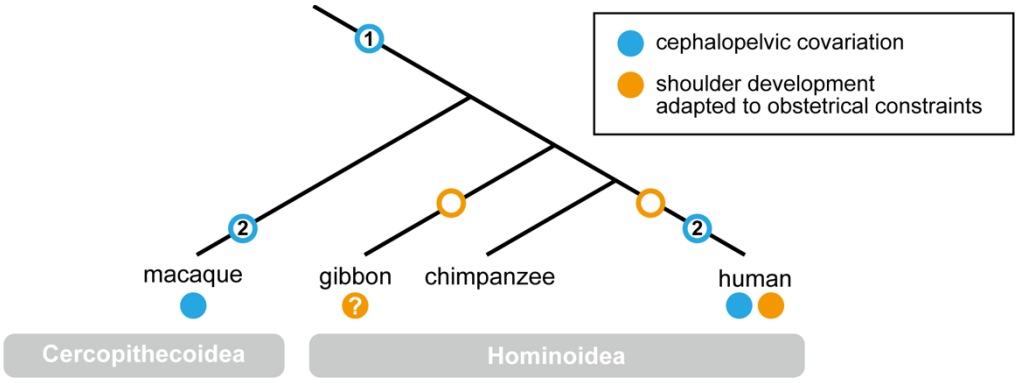

Fig. 4.1 The evolutionary scenarios for obstetrical adaptations in primates. Closed circles in light blue and orange color indicate presence of the cephalopelvic covariation and obstetrically relevant shoulder development, respectively. Light blue and orange open circles indicate evolutionary scenarios. Scenarios 1 and 2 indicate possibilities that cephalopelvic covariation was present already in early catarrhines and that it was acquired independently in humans and macaques, respectively. Gibbons might have human-like shoulder development as an adaptation to their obstetrical constraints, which should remain to be tested.

There are two possible evolutionary scenarios. The first is that the cephalopelvic covariation was present already in early catarrhines, and the second is that it was obtained independently in each lineage (parallel evolution). According to the first scenario, the obstetrical adaptations found in modern humans in the head and shoulders have different evolutionary foundations. While a feature found in the shoulder development (perinatal growth depression) is likely to be a derived feature for humans, the cephalopelvic covariation could have a deeper evolutionary root. If this is the case, the cephalopelvic covariation was already "prepared" for humans in advance of marked encephalization. Contrastingly, the feature in the shoulders evolved only when the shoulders became wide relative to the birth canal in humans. Whether or not perinatal growth depression is unique to humans should, however, be tested by further studies (see below). According to the second scenario, the obstetrical adaptations in the head and shoulders of modern humans could have been brought more closely to each other during human evolution than in the case of the first scenario. How large was the time lag between the two? DeSilva et al. (2017) proposed that *Australopithecus afarensis*, dating back to ~3 mya, could have had tight fit between the neonatal shoulder and maternal birth canal which indicate an elevated risk of the shoulder dystocia. *A. afarensis* was not as large brained as modern humans (Falk et al., 2009; Falk et al., 2000), and thus the cephalopelvic proportion is estimated to be smaller than in modern humans (DeSilva et al., 2017; Häusler & Schmid, 1995; Tague & Lovejoy, 1986). This

indicates a possibility that humans evolved features to mitigate the obstetrical constraints in the shoulders earlier than in the head. On the other hand, investigation of the Taung skull using medical imaging showed that *A. africanus* exhibited a delayed fusion of the metopic suture (Falk et al., 2012) [but see Holloway et al. (2014)]. This might indicate that obstetrical adaptations of the head and shoulders evolved in concert. Further data of fossil hominins are necessary to identify how closely the head and shoulder features to mitigate obstetrical constraint evolved in humans.

The obstetrical dilemma hypothesis proposes that functions of delivery and locomotion are in conflict (Pavličev et al., 2020; Stansfield et al., 2021; Washburn, 1960). Data of cephalopelvic covariation show that the macaque pelvis provides a "solution" to the dilemma by splitting the pelvis into functional units of delivery and locomotion (Fig. 4.2). Such a separation of functional units is also found in the skeletal parts other than the pelvis (Fig. 4.2). Data of shoulder and pelvic development show that, in humans, the clavicle, a part of the upper-limb girdle, exhibits growth depression, while the pelvis, the lower-limb girdle, does not exhibit such a pattern (Fig. 3.2). Likewise, long bones follow different ontogenetic patterns from the clavicle (Fig. 3.2). It is interesting to note that the elongation of the hind-limbs in humans on one hand and that of forelimbs in chimpanzees on the other, which do not primarily cause obstetrical difficulties, are not developmentally constrained. It has been proposed that the pelvic morphology exhibits a developmental modification according to obstetrical versus locomotor demands during the lifetime of human females (Huseynov et al., 2016). My data add to the evidence that the obstetrical constraint has more pervasive effects on phenotypic features of humans than previously thought, and that such effects are found not only for humans, but also for other primate taxa that have obstetrical constraint (Fig. 1.2). For example, covariation could be found in other skeletal parts. The shoulder data showed shoulder width grows isometrically with cranial length during fetal period (Fig. 3.4). Since neonatal head and maternal pelvic morphologies covary with each other in macaques and possibly in humans, it is likely that neonatal shoulder and maternal birth canal dimensions also show a covariation. This hypothesis, however, should remain to be tested by actualistic data.

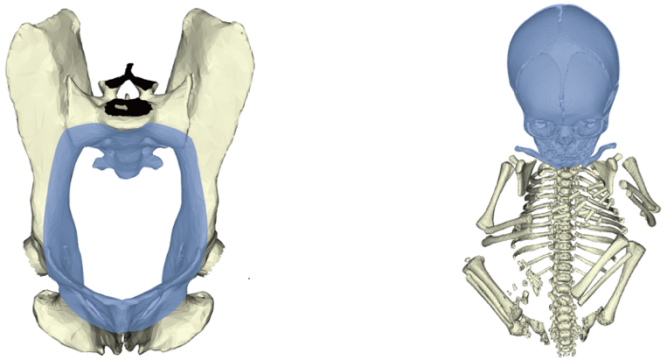

Fig. 4.2 Modularity adaptations to obstetrical constraints in maternal and fetal sides. Fetopelvic covariation is strongly expressed in birth canal (chapter 2), and developmental adaptations for obstetrical constraints are shown only in skull and clavicle (chapter 3).

Primates show variation of proportion between maternal birth canal and neonatal head and shoulders (Fig. 1.2) (Schultz, 1949) Extensive data from wide range of primate taxa are of special relevance in various respects. For example, data from great apes would be important to test the hypothesis that the cephalopelvic covariation was present already in early catarrhines. Gibbons are also important. Gibbons exhibit a tight fit between the neonatal shoulder width and maternal pelvic dimension (Fig. 1.2) (Schultz, 1949). Data of gibbons would give insights into whether the perinatal growth depression is specific to humans. Further challenges are to identify the mechanism at the genetic level and to understand whether the observed patterns represent long-term adaptation. For the former, rhesus macaques would play an important role. Pattern of fetopelvic covariation exhibited in rhesus macaques suggest that mechanism behind cephalopelvic covariation could be shared among primates, but its expression pattern would be related species-specific obstetrical conditions. For the latter, constructing the evolutionary models that incorporates taxon-specific ontogenetic patterns would be an interesting challenge.

References

DeSilva, J. M., Laudicina, N. M., Rosenberg, K. R., & Trevathan, W. R. (2017). Neonatal shoulder width suggests a semirotational, oblique birth mechanism in *Australopithecus afarensis*. *The Anatomical Record, 300*(5), 890-899. doi:10.1002/ar.23573

Falk, D., Hildebolt, C., Smith, K., Morwood, M. J., Sutikna, T., Jatmiko, Wayhu Saptomo, E., & Prior, F. (2009). LB1's virtual endocast, microcephaly, and hominin brain evolution. *Journal of Human Evolution, 57*(5), 597-607.

doi:https://doi.org/10.1016/j.jhevol.2008.10.008

Falk, D., Redmond, J. C., Guyer, J., Conroy, C., Recheis, W., Weber, G. W., & Seidler, H. (2000). Early hominid brain evolution: a new look at old endocasts. *Journal of Human Evolution, 38*(5), 695-717. doi:https://doi.org/10.1006/jhev.1999.0378

Falk, D., Zollikofer, C. P. E., Morimoto, N., & Ponce de León, M. S. (2012). Metopic suture of Taung (*Australopithecus africanus*) and its implications for hominin brain evolution. *Proceedings of the National Academy of Sciences, 109*(22), 8467-8470. doi:10.1073/pnas.1119752109

Fischer, B., & Mitteroecker, P. (2015). Covariation between human pelvis shape, stature, and head size alleviates the obstetric dilemma. *Proceedings of the National Academy of Sciences, 112*(18), 5655-5660. doi:10.1073/pnas.1420325112

Häusler, M., & Schmid, P. (1995). Comparison of the pelves of Sts 14 and AL288-1: implications for birth and sexual dimorphism in australopithecines. *Journal of Human Evolution, 29*(4), 363-383. doi:https://doi.org/10.1006/jhev.1995.1063

Holloway, R. L., Broadfield, D. C., & Carlson, K. J. (2014). New high-resolution computed tomography data of the Taung partial cranium and endocast and their bearing on metopism and hominin brain evolution. *Proceedings of the National Academy of Sciences, 111*(36), 13022-13027. doi:10.1073/pnas.1402905111

Huseynov, A., Zollikofer, C. P. E., Coudyzer, W., Gascho, D., Kellenberger, C., Hinzpeter, R., & Ponce de León, M. S. (2016). Developmental evidence for obstetric adaptation of the human female pelvis. *Proceedings of the National Academy of Sciences, 113*(19), 5227-5232. doi:10.1073/pnas.1517085113

Pavličev, M., Romero, R., & Mitteroecker, P. (2020). Evolution of the human pelvis and obstructed labor: new explanations of an old obstetrical dilemma. *American Journal of Obstetrics & Gynecology, 222*(1), 3-16. doi:10.1016/j.ajog.2019.06.043

Schultz, A. H. (1949). Sex differences in the pelves of primates. *American Journal of Physical Anthropology, 7*(3), 401-424. doi:10.1002/ajpa.1330070307

Stansfield, E., Kumar, K., Mitteroecker, P., & Grunstra, N. D. S. (2021). Biomechanical trade-offs in the pelvic floor constrain the evolution of the human birth canal. *Proceedings of the National Academy of Sciences, 118*(16), e2022159118.

doi:doi:10.1073/pnas.2022159118

Tague, R. G., & Lovejoy, C. O. (1986). The obstetric pelvis of A.L. 288-1 (Lucy). *Journal of Human Evolution, 15*(4), 237-255. doi:https://doi.org/10.1016/S0047-2484(86)80052-5

Washburn, S. L. (1960). Tools and human evolution. *Scientific American, 203*(3), 62-75.

Acknowledgements

I would like to express my gratitude to Prof. Masato Nakatsukasa and Prof. Naoki Morimoto for their generous and thoughtful support during the study. I am grateful to Dr. Takeshi Nishimura, Dr. Akihisa Kaneko, Dr. Naomichi Ogihara, Dr. Shigehito Yamada, Dr. Walter Coudyzere, Dr. Christoph P. E. Zollikofer, and Dr. Marcia S. Ponce de León for constructive comments and suggestions. I thank Dr. Wataru Morita and Mr. Satoshi Kobayashi for giving comments on statistical analyses and Dr. Kazumichi Katayama for his encouragement. I thank Dr. Brian Shearer for proofreading the manuscript. I also thank Dr. Yutaka Kunimatsu, Mr. Yuma Tomizawa, and Ms. Akiko Yoshimura and members of Laboratory of Physical Anthropology for their help and discussions on my study. I thank the staff of the Center for Human Evolution Modeling Research at KUPRI for assistance in this thesis and daily care of the monkeys. I thank Dr. Peter Jans for help with CT scanning. I also appreciate the Great Ape Information Network project and Tennoji Zoo for their help in collecting great ape specimens. This thesis was supported in part by Cooperative Research Program at KUPRI Grants, Japan Society for the Promotion of Science KAKENHI, and the strategic research partnership between Kyoto University and the University of Zurich. Last but not least, I would like to thank my family for an invaluable support throughout my study.